data suggest that fibronectin is a key molecule involved in the overexpression of $P2X_4$ in microglia after nerve injury.

In the present study, we demonstrate that: (1) culturing primary microglia on fibronectin induces the upregulation of functional $P2X_4$ receptors on the cell surface in vitro, (2) increased expression of fibronectin was observed in the ipsilateral side of the spinal cord taken from allodynia rats, and (3) intrathecal administration of ATP-stimulated microglia that had been treated with fibronectin enhanced the allodynic response in rats in vivo. All these findings suggest that the increase in spinal fibronectin after a spinal nerve injury is a critical event in the upregulation of microglial $P2X_4$ receptors, which would be important for the onset of mechanical allodynia.

MATERIALS AND METHODS

Isolation of Microglia

The primary cultures of rat microglia were derived from the forebrains of neonatal Wistar rats (Nakajima et al., 1992). In brief, the rat cortices were separated from the meninges, minced, treated with trypsin and with DNase, and then centrifuged to remove dead cells. The pellet was resuspended in DMEM, filtrated, and cultured in medium with 10% fetal bovine serum for 12–23 days. Microglia were isolated on day 10 and day 15 by gently shaking the flasks for 2 min.

Quantitative RT-PCR

Microglia were plated on tissue culture dishes that had been coated with fibronectin (Sigma, Missouri, USA) at 10 μg/ml or non-treated, and kept at 37°C for 3 h. Then, the cells were washed with warm DMEM twice and the total RNA was extracted using the RNeasy mini kit (QIAGEN Japan, Tokyo, Japan). Real time RT-PCR was performed using the TaqMan One-Step RT-PCR Master Mix Kit (Applied Biosystems, CA), $P2X_4$ primers, and TaqMan GAPDH Control Reagents (Applied Biosystems). The forward and reverse primer pairs for $P2X_4$ were:

F: 5′-TGGCGGACTATGTGATTCCA-3′

R: 5′-GGTTCACGGTGACGATCATG-3′

The PCR reaction was carried out by One Step RT-PCR in a total volume of 25 μl using the ABI PRISM 7700 Sequence Detection system (Applied Biosystems). All values were normalized with the GAPDH expression.

Western Blotting

Microglia were lysed in lysis buffer (50 mM Tris-HCl pH 7.4, 150 mM NaCl, 1% NP-40, 1% SDS, 5 mM EDTA, protease inhibitors cocktail) and mixed with Laemmli sample buffer. For the rat spinal cord homogenates, the L5 corresponding spinal cord was collected from control or allodynia rats of 1-, 3-, 7-day post operation and the area of dorsal horn was excised. Then the tissue was homogenized in homogenization buffer (PBS, 1% NP-40, 1% Triton X-100, 5mM EDTA, protease inhibitors cocktail) for 20 s on ice, centrifuged thoroughly to remove cell debris, and mixed with Laemmli sample buffer. All samples were subject to BCA assay to adjust the loading protein amount. Cell lysates or tissue homogenates were resolved by SDS-PAGE and transferred to nitrocellulose membrane (BioRad, CA). The membrane was blocked with TBS-Tween 0.05%, 1% BSA, 0.02% NaN_3, and probed with primary antibodies: anti-$P2X_4$ (Alomone, Jerusalem, Israel, 1:200 dilution), anti-β-actin (Sigma, 1:1000 dilution), anti-ERK2 (Santa Cruz, CA, 1:200 dilution), or anti-fibronectin (Dako, Glostrup, Denmark, 1:100 dilution). The antibodies were detected using horseradish peroxidase-conjugated anti-rabbit and anti-mouse IgG secondary antibodies (Amersham Biosciences, NJ, 1:1000 dilution) and visualized with the ECL system (Amersham Biosciences). Bands were quantified using NIH Image J 1.33u software.

Intracellular Calcium Concentration ($[Ca^{2+}]i$) Measurement

Microglia were cultured for 24 h at 37°C on an appropriately coated Flexiperm cover glass. Then the culture medium was replaced with balanced salt solution (BSS at pH 7.4: 150 mM NaCl, 5 mM KCl, 1.8 mM $CaCl_2$, 1.2 mM $MgCl_2$, 25 mM HEPES, 10 mM D-glucose). Cells were loaded with fura-2 by incubating them with 5 μM fura-2-acetoxymethylester in BSS for 1 h at room temperature. Changes in $[Ca^{2+}]i$ were assessed by ratiometric images (F340/F380) of fura-2 fluorescence, which were detected with Aquacosmos/HiSca (Hamamatsu Photonics, Hamamatsu, Japan). For TNP-ATP(100 μM), PPADS (10 μM), or 0 Ca^{2+} (removal of extracellular Ca^{2+}) experiments, cells were treated with these antagonists or the 0 Ca^{2+} solution 2 min before and during ATP-applications.

Chung Model

All experiments were performed using 8-week-old male Wistar rats. All surgeries were performed under inhalation anesthesia using Forene in 100% O_2, induced at 5% and maintained at 2%. The spinal nerve on the left side was exposed at a proximal location under an aseptic condition. Then the 5^{th} lumber spinal nerve was tightly ligated with a silk suture (5-0) and its peripheral side was completely transected. The muscle and the skin were sutured closed, and the animal was allowed to recover before the behavioral testing. To evaluate allodynia, von Frey filaments were applied to the plantar surface of the hindpaw, and the withdrawal from mechanical stimulus was monitored as previously reported (Tsuda et al., 2003).

Intrathecal Catheterization and Injections of Microglia

For intrathecal microglia administration, intrathecal catheterization was performed on Wistar rats (12 weeks, male) (Tsuda et al., 2003). Briefly, with the rat under inha-

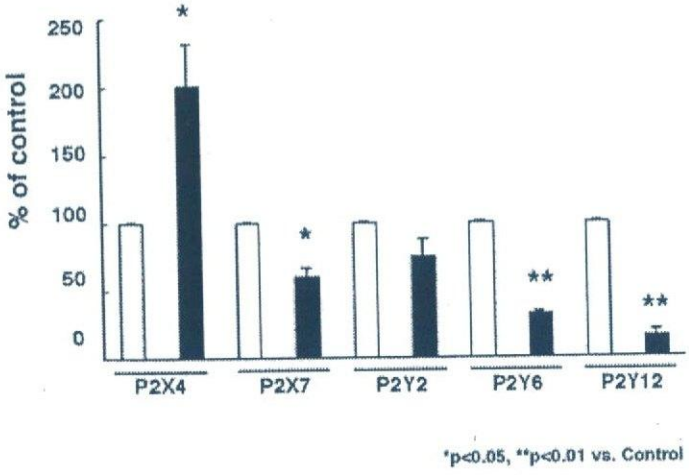

Fig. 1. The effect of fibronectin on the mRNA expression of microglial $P2X_4$. Fibronectin increased the expression of $P2X_4$ in microglia at the mRNA level. Microglia were cultured on fibronectin for 3 h at 37°C, and the expression of $P2X_4$ was assessed by quantitative RT-PCR. $P2X_4$ was markedly upregulated by fibronectin, whereas the mRNA expressions of $P2X_7$, $P2Y_2$, $P2Y_6$, and $P2Y_{12}$ purinoreceptors were significantly decreased. Data are mean ± SE of 3 separate experiments. Asterisks show significant difference from control (*$P < 0.05$, ** $P < 0.01$ vs. control, Student's t-test).

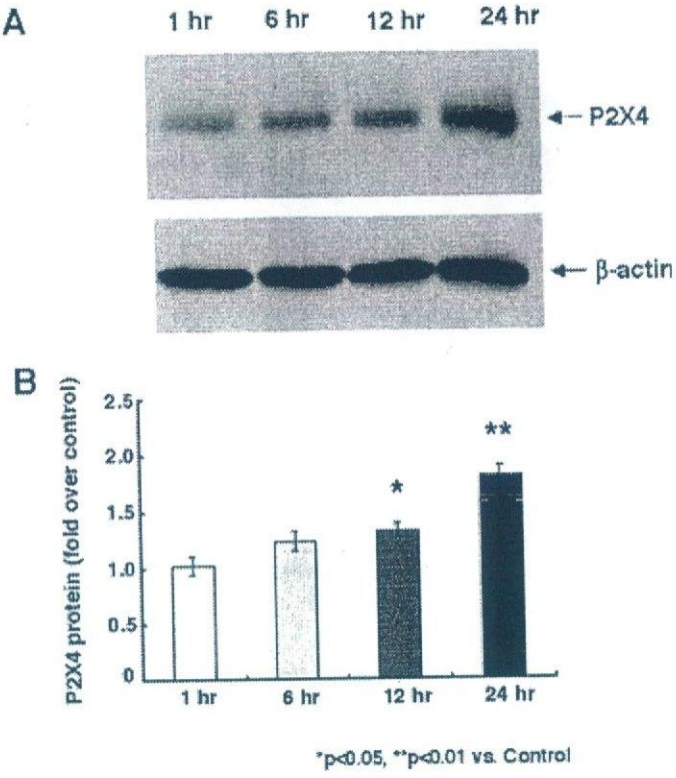

Fig. 2. Time-course study of the microglial $P2X_4$ upregulation. Fibronectin increased the expression of $P2X_4$ in microglia at the protein level. Microglia were cultured on fibronectin for 1, 6, 12, and 24 h at 37°C, and the protein expression of $P2X_4$ receptors was analyzed by Western blotting. The protein expression of $P2X_4$ receptors began to increase after 12 h of incubation and increased strongly after 24 h of incubation. The intensity of the bands was quantified with a computing densitometer using NIH Image J 1.33u image analysis software. Asterisks show significant difference from control (*$P < 0.05$, ** $P < 0.01$ vs. control, Student's t-test).

lation anesthesia, an incision was made in the atlanto-occipital membrane and the catheter was inserted caudally to the lumber enlargement (close to L4-L5 segments) of the spinal cord. Verification of the catheter placement was made by the observation of hind limb paralysis after intrathecal injection of lidocaine (2%, 5 μl) 3 days after catheterization. Animals that failed the verification for the catheter placement were not included in the data analyses. Microglia were cultured on uncoated- or fibronectin-coated dishes for 24 h at 37°C, washed twice with PBS, and harvested. After adjusting their concentrations, cells were stimulated with ATP at 0, 0.5, and 5 μM, incubated for 1 h at 37°C, and subsequently microinjected. Animals were subject to the behavioral testing 5 h after the injection.

Statistical Analysis

The von Frey test results were analyzed by the Mann-Whitney U-test and values with $P < 0.05$ were considered statistically significant. For the other data, the Student's t test was performed, and values with $P < 0.05$ (or $P < 0.01$ where appropriate) were considered statistically significant as compared to controls.

RESULTS

Fibronectin Increased the Expression of $P2X_4$ Receptors in Microglia at both the mRNA and Protein Levels

Microglia were plated onto fibronectin or control plastic, and their P2 receptor expression was studied by quantitative RT-PCR (Fig. 1). To normalize the results, we used the mRNA expression of glyceraldehyde-3-phosphate dehydrogenase (GAPDH) as the endogenous control and, therefore, the P2 receptor gene expression was given as the ratio P2X(Y)/GAPDH. As shown in the figure, incubation of microglia on fibronectin at 10 μg/ml for 3 h resulted in the marked upregulation of $P2X_4$ gene expression, whereas the mRNA expressions of $P2X_7$, $P2Y_2$, $P2Y_6$, and $P2Y_{12}$ were all rather diminished (Fig. 1), suggesting that the $P2X_4$ receptor is unique among the purinoceptors on microglia.

To confirm this effect of fibronectin on the $P2X_4$ receptor at the protein level, we examined its expression by Western blotting using anti-$P2X_4$ antibody (Fig. 2). As seen in Fig. 2, microglial $P2X_4$ appeared as a single band at ~75 kDa, and since its predicted molecular weight from its protein sequence is 43 kDa, the molecule seems to be heavily glycosilated (Soto et al., 1996). We previously reported that fibronectin induces profound microglial proliferation through β1 integrin (Nasu-Tada et al., 2005), and thus the protein amount loaded on the gel was carefully adjusted. In addition, β-actin was used as the endogenous control to normalize the Western blot data. Each band was quantified using computing software, and the basal value of β-actin was subtracted from the $P2X_4$ results. The increase in $P2X_4$ expression became evident after 12 h of fibronectin stimulation (Fig. 2) (1.3-fold as compared to 1 h incubation, $P < 0.05$), and the increase continued until it reached an

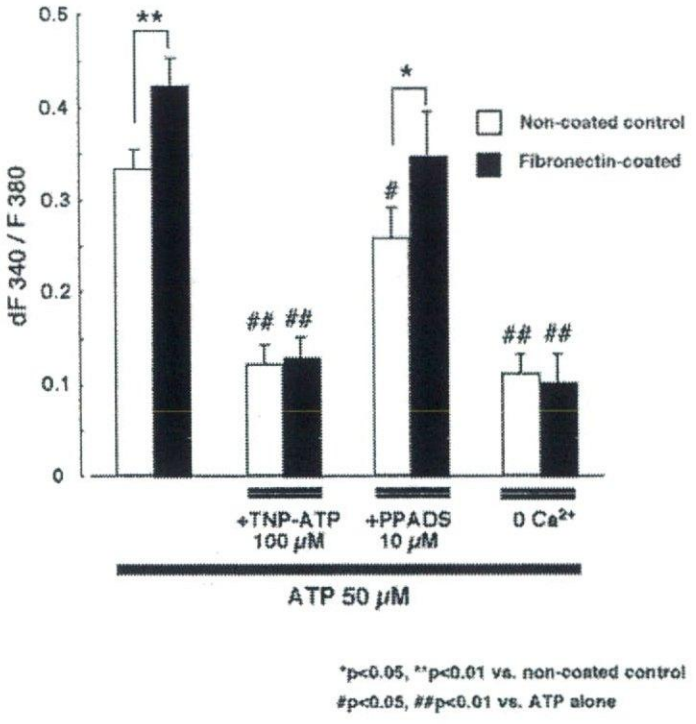

Fig. 3. Enhancement by fibronectin of the function of $P2X_4$ receptors in microglia. The function of microglial $P2X_4$ was assessed by fura-2 based $[Ca^{2+}]i$ imaging (ratio of F340/F380). Microglia cultured on fibronectin showed an increase in the Ca^{2+} response to stimulation with ATP 50 μM. Microglia were cultured for 24 h on fibronectin or on a control, and pretreated with TNP-ATP (100 μM) or PPADS (10 μM) for 2 min where required. Flexiperm cover glass (i.e., non-coated) and the ATP (50 μM)-evoked increase in $[Ca^{2+}]i$ was monitored. 0 Ca^{2+} indicates removal of Ca^{2+} from the extracellular medium. Asterisks and #s show significant difference from non-coated control and ATP alone, respectively (*$P < 0.05$, ** $P < 0.01$ vs. control; # $P < 0.05$, ## $P < 0.01$ vs. ATP alone, Student's t-test).

approximately 2-fold increase after 24 h incubation ($P < 0.01$).

Microglia Cultured on Fibronectin Showed an Increase in $[Ca^{2+}]i$ in Response to ATP Stimulation

To confirm that fibronectin upregulates functional $P2X_4$ receptors on microglia, the ATP-evoked increases in $[Ca^{2+}]i$ were subsequently studied. Microglia were cultured for 24 h on fibronectin or on uncoated Flexiperm cover glass (control), and the changes in $[Ca^{2+}]i$ in response to ATP (50 μM) were detected by the conventional fura-2 method., i.e., the ratiometric images of fura-2 fluorescence. The nucleotide receptors that are known to be expressed in microglia include $P2X_4$, $P2X_7$, $P2Y_2$, $P2Y_6$, $P2Y_{12}$ (Inoue, 2002; Sasaki et al., 2003; Tsuda et al., 2003), and possibly $P2Y_{13}$ due to its abundant mRNA in the brain and the immune system (Zhang et al., 2002). $P2Y_{12}$ and $P2Y_{13}$ receptors are Gi-coupled P2 receptors, and the activation of these receptors, in general, does not cause an elevation in $[Ca^{2+}]i$ but decreases the intracellular cAMP.

In the absence of extracellular Ca^{2+} (Fig. 3, 0 Ca^{2+}), neither the control nor microglia cultured with fibronectin showed much response to ATP 50 μM stimulation, suggesting that Gq/11-phospholipase C coupled P2Y receptors, which are dependent on intracellular Ca^{2+} storage, were not relevant to this case. In contrast, in the presence of extracellular Ca^{2+}, microglia on fibronectin showed a significant increase ($P < 0.01$) in the Ca^{2+} response to ATP 50 μM (Fig. 3, ATP alone), indicating that the expression of the ion-channel type purinoceptors, i.e., P2X receptors, is augmented by fibronectin and that these are likely to be $P2X_4$ receptors, since the $P2X_7$ receptor is activated at a relatively high concentration of ATP (i.e., concentrations greater than 100 μM) (Ralevic and Burnstock, 1998). Pretreatment of cells with TNP-ATP (an antagonist of $P2X_{1-4}$ receptors) dramatically reduced the $[Ca^{2+}]i$ response in microglia on both control and fibronectin-coated dishes, indicating that basal response to ATP at 50 μM as well as its augmented response on fibronectin substrate mostly result from microglial $P2X_4$ receptor. On the other hand, pretreatment with PPDAS (an antagonist of $P2X_{1,2,3,5,7}$) did not fundamentally affect but only slightly reduced the $[Ca^{2+}]i$ response in both populations. PPADS is known to inhibit $P2Y_{1-2}$ receptors as well and, therefore, the result indicates that microglial $P2Y_2$ receptor also constitutes the $[Ca^{2+}]i$ response to ATP stimulation. In conclusion, fibronectin upregulated the functional $P2X_4$ receptors on the microglial surface, and this lead to an enhancement of the increase in $[Ca^{2+}]i$ evoked by ATP 50 μM via $P2X_4$ receptors.

Fibronectin Was Upregulated in the Allodynia Rat Spinal Cord

As described earlier, the importance of the microglial $P2X_4$ receptor in the induction of mechanical allodynia after nerve injury has recently become evident (Tsuda et al., 2003). We sought to determine the profile of fibronectin expression in the spinal cord of nerve-injured rats, where the microglial $P2X_4$ receptor expression is increased. L5 spinal cord segments were harvested from rats of control, 1-, 3- and 7-day post nerve injury, and the expression of fibronectin was assessed by Western blotting. There has been little evidence for fibronectin in the normal CNS other than in the basement membrane of endothelial, pial, and ependymal cells, and our result showed that Naive and Day 1 rats exhibited slight signs of fibronectin (Fig. 4). However, spinal fibronectin became evident on the ipsilateral side at 3 and 7 days following the nerve injury (Fig. 4, Day 3 ipsi, Day 7 ipsi). The contralateral side remained unchanged throughout the experiment.

Upregulation of Microglial $P2X_4$ Receptors Lowered the Threshold of Pain Responses Caused by Intrathecal Transfer of the Cells

In the study by Tsuda et al. (2003), the intrathecal transfer of ATP-treated microglia induced mechanical allodynia

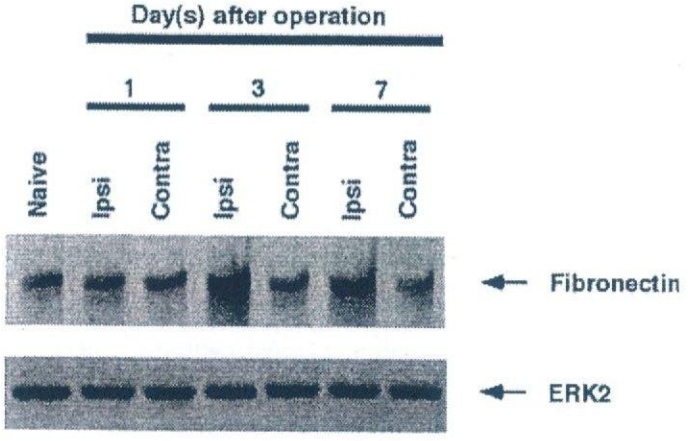

Fig. 4. Time-course study of fibronectin expression in the allodynia rat spinal cord. The rat spinal nerve on the left side was exposed, tightly ligated with a silk suture, and its peripheral side was completely transected. On Days 1, 3, and 7 post-operation, L5 spinal cords from control and allodynia rats were collected and the tissues were subjected to homogenization and Western blotting. Anti-fibronectin (Dako, 1:100 dilution) antibody and HRP-conjugated anti-rabbit IgG (Amersham) antibody were used for the detection. The data represent 3 independent experiments.

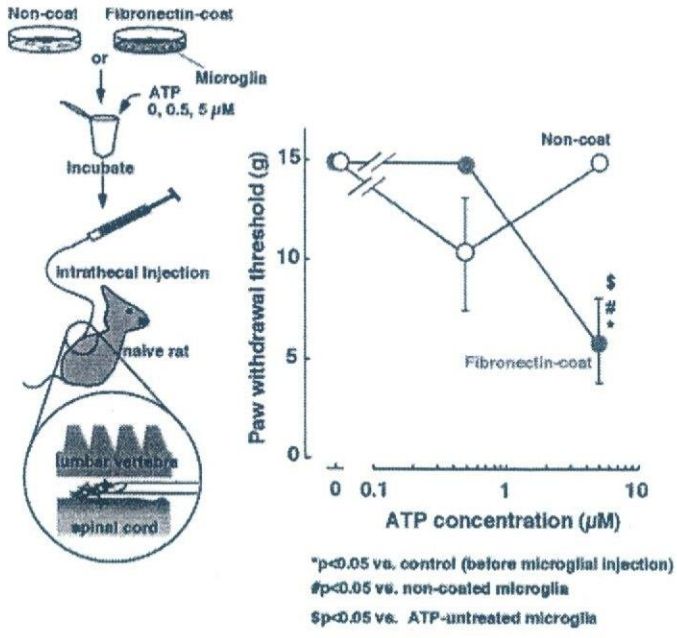

Fig. 5. Changes in nociceptive response after intrathecal transfer of microglia with elevated expression of P2X$_4$ receptors. Microglia were cultured either on fibronectin (red circle) or on control plastic (white circle) for 24 h at 37°C and both groups were subsequently stimulated with ATP at 0 (control), 0.5, and 5 μM for 1 h at 37°C. Without intrathecal microinjection of microglia, no rats showed pain behavior. Then the cells were intrathecally transferred to the lumbosacral spinal cord of a normal rat. Five h after the microinjection, nociceptive responses were evaluated by measuring the 50% paw withdrawal threshold to mechanical stimuli. Six rats were used in each group for this study. The Mann-Whitney U-test was performed and statistical significance was set at $P < 0.05$ [$^*P < 0.05$ vs. control (before microglial injection); $\#P < 0.05$ vs. non-coated microglia; $\$P < 0.05$ vs. ATP-untreated microglial injection]. [Color figure can be viewed in the online issue, which is available at www.interscience.wiley.com.]

in normal rats, and microglial P2X$_4$ receptors were mainly responsible for this effect. Therefore, we hypothesized that microglia with more P2X$_4$ receptors expressed on the surface are capable of causing severer mechanical allodynia. To examine this hypothesis, microglia were cultured either on fibronectin or on control plastic for 24 h, stimulated with 0.5 or 5 μM of ATP for 1 h or left untreated as the control, then intrathecally transferred to normal rats, and their pain behavior was monitored 5 h after the microinjection using von Frey hairs to calculate the 50% paw withdrawal threshold (Fig. 5). Without intrathecal injection of microglia, no rat showed any pain behavior (data not shown). As seen in Fig. 5, no pain response was observed at ATP 0 (control) or 0.5 μM. An interesting difference, however, was seen at ATP 5 μM, where a significant decrease in the 50% withdrawal threshold was observed with fibronectin-treated microglia as compared with the non-treated microglia. Additionally, it was clearly demonstrated that intrathecal transfer of microglia that were treated with ATP at 50 μM, in the absence of fibronectin, was capable of inducing allodynia in the recipient rat (Tsuda et al., 2003). Collectively, these results suggest that upregulation of P2X$_4$ receptors by fibronectin lowered the threshold for the response to mechanical allodynia.

DISCUSSION

In the present study, we demonstrated that: (1) the treatment of microglia with fibronectin enhanced the expression of functional P2X$_4$ receptors, (2) the spinal fibronectin was upregulated after the peripheral nerve injury, and (3) the fibronectin treatment of microglia lowered the concentration of ATP that was necessary to cause mechanical allodynia by intrathecal transfer. Because the upregulation of P2X$_4$ receptors in spinal microglia is a critical event in the induction of mechanical allodynia after peripheral nerve injury (Tsuda et al., 2003, 2005), our present results may partially clarify the mechanism of mechanical allodynia.

The Correlation Between Fibronectin and Microglial P2X$_4$ Receptor

The P2X$_4$ receptor displays a broad tissue distribution, especially in the CNS (Soto et al., 1996). Although the precise physiological roles of P2X$_4$ receptors remain unknown, it has been reported that the upregulation of P2X$_4$ receptors is linked to several pathological conditions, such as nerve injury (Tsuda et al., 2003), ischemia (Cavaliere et al., 2003), and muscular dystrophy (Yeung et al., 2004). In the present study, we showed that fibronectin increased the microglial P2X$_4$ expression at the mRNA level by more than 2-fold. The elevation was also confirmed at the protein level, and these upregulated P2X$_4$ receptors were shown to be functional by the increase in $[Ca^{2+}]i$ mediated by P2X$_4$ receptors.

These findings are of interest because some ECM molecules, including fibronectin, are known to be upregulated following adult CNS injury (Jones, 1996). Fibro-

nectin is involved in neurite growth during development (Matthiessen et al., 1989) and plays an important role in the spinal cord development in humans (Krolo et al., 1998). The expression of fibronectin is regionally and developmentally regulated in the brain, and its presence is relatively minor in the normal CNS (Jones, 1996). However, once injuries occur, its expression is dramatically increased (Hoke and Silver, 1996; Pasinetti et al., 1993). Fibronectin also exists at high concentrations in the blood plasma, and a breakdown of the blood-brain barrier (BBB) should result in an increase in its local concentration in the CNS. Thus, it is highly plausible that the increased fibronectin may somehow upregulate $P2X_4$ receptors in microglia.

The signaling pathway(s) by which fibronectin promotes $P2X_4$ upregulation is currently under investigation. Microglia possess functional β1 integrin, which is one of the receptors for fibronectin, and they undergo firm adhesion, activation (Milner and Campbell, 2002, 2003), and proliferation (Nasu-Tada et al., 2005) through this molecule, presumably by regulating intracellular signaling cascades. Thus, fibronectin-to-integrin-mediated signals may be critical for the $P2X_4$ receptor upregulation. It is interesting that, among various P2 receptors expressed in microglia, i.e., $P2X_7$, $P2Y_2$, $P2Y_6$, and $P2Y_{12}$ receptors, only the $P2X_4$ receptor is upregulated by fibronectin (Fig. 1). This result suggests that the $P2X_4$ receptor gene may undergo unique transcriptional regulation by the linkage of fibronectin to integrin.

The Correlation Between Spinal Fibronectin and Mechanical Allodynia in Rats

We showed that spinal fibronectin was upregulated after the nerve injury. Several lines of evidence indicate that fibronectin is directly upregulated at the site of injuries in the PNS (Lefcort et al., 1992; Martini, 1994; Vogelezang et al., 1999) and CNS (Hoke and Silver, 1996; Pasinetti et al., 1993); but to our knowledge, there has been no report demonstrating that fibronectin is upregulated at a distal region, i.e., in the CNS, after peripheral nerve injury. The clinical signs of allodynia induced in rat in the Chung model become evident by 3-day post operation and the phenotype reached the maximum by 1-week post operation. The concomitant upregulation of the microglial $P2X_4$ receptors, which is observed only on the ipsilateral side of the spinal cord, follows the same time-course profile (Tsuda et al., 2003). In this study, the expression of the spinal fibronectin was strongly augmented, but again only on the ipsilateral side, during the course of mechanical allodynia, and the expression pattern was also similar to the time-course of the above. Therefore, our results strongly suggest that the upregulation of the ipsilateral fibronectin correlates both with the induction of allodynia and with the upregulation of the microglial $P2X_4$ receptor. Since it is usually observed that mechanical allodynia spans several weeks, it is still necessary for us to investigate the relationship between the upregulation of fibronectin and chronic allodynia. Our data so far postulate that fibronectin may be involved in the onset of the disease, most likely by initiating the upregulation of the microglial $P2X_4$ receptor.

Since fibronectin is known to be present at a high concentration in the blood plasma, it is plausible that the peripheral nerve injury caused a local breakdown of the central BBB, and that the breakdown resulted in a transfer of the blood plasma fibronectin into the corresponding part of the CNS. In a cortical cold-injury model, fibronectin was found to leak from blood vessels (Nag et al., 2001; Nourhaghighi et al., 2003); but in another report, such exudation was not seen after spinal cord injury (Farooque et al., 1992). Interestingly, the plasma fibronectin expression is known to be elevated after tissue injury (Thompson et al., 1992). Recently, plasma fibronectin was reported to support neuronal survival and reduce bran injury following transient focal cerebral ischemia, but it was not essential for skin-wound healing and hemostasis (Sakai et al., 2001). Alternatively, fibronectin may be synthesized by neuronal and glial cells in the CNS. Fibronectin is a vital molecule in neural development and regeneration (Venstrom and Reichardt, 1993), and astrocytes are known to synthesize and release fibronectin (Jiang et al., 1994; Matthiessen et al., 1989; Price and Hynes, 1985). A recent report by Tom et al. (2004) revealed that astroglial-associated fibronectin plays a key role in axonal regeneration in the white matter and, indeed, astrocytes produce and release fibronectin in response to ATP stimulation (unpublished observation). However, so far we have not identified the source of the upregulated fibronectin, and the mechanism by which fibronectin is upregulated after peripheral nerve injury remains to be clarified.

The effect of fibronectin was further highlighted by the experiment involving intrathecal transfer. In our previous study (Tsuda et al., 2003), microglia that were treated with 50 μM ATP could induce mechanical allodynia when they were intrathecally transferred into a normal rat. Microglia that were cultured on fibronectin and treated with 5 μM ATP were capable of inducing mechanical allodynia. In contrast, control microglia were not able to induce mechanical allodynia at that ATP concentration. The result suggests that fibronectin lowered the threshold of pain sensation. Fifty μM of ATP was adequate to cause mechanical allodynia by intrathecal transfer in both groups, suggesting that the effect of microglia in causing allodynia in response to ATP stimulation is saturated at an ATP concentration of 50 μM. Although microglia have other P2 receptors, i.e., $P2X_7$, $P2Y_2$, $P2Y_6$, and $P2Y_{12}$ receptors, only $P2X_4$ receptors are involved in the induction of mechanical allodynia (Tsuda et al., 2003). Interestingly, fibronectin upregulated only $P2X_4$ receptors but downregulated other P2 receptors on microglia at the mRNA level (Fig. 1). Thus, the involvement of other microglial P2 receptors in pain sensation, the threshold of which was lowered by fibronectin, would be negligible. Altogether, the results suggest that microglia with upregulated $P2X_4$ receptors by fibronectin treatment were able to transduce signals that lead to allodynia at a lower concentration of ATP.

In summary, we demonstrated that fibronectin induces the upregulation of $P2X_4$ receptors on microglia in vitro, and that fibronectin is increased in the spinal cord in vivo when mechanical allodynia is induced after peripheral nerve injury. When microglia are intrathecally administered into normal rats, they induce mechanical allodynia only if pre-stimulated with ATP (Tsuda et al., 2003). Our ex vivo experiments showed that fibronectin lowers the ATP concentration that is necessary for microglia to induce this pain behavior. Although both the signaling pathway by which fibronectin promotes $P2X_4$ upregulation and the source of increased fibronectin are currently under investigation, all these findings suggest that the upregulation of spinal fibronectin may be involved in the onset mechanism of mechanical allodynia after nerve injury.

ACKNOWLEDGMENTS

We thank Dr. Ohno for continuous encouragement. This study was partly supported by an MF-16 grant from The National Institute of Biomedical Innovation, a grant from Uehara Memorial Foundation, a grant-in-aid for Scientific Research (B), for Young Scientists (A) and on Priority Areas (A) from the Ministry of Education, Science, Sports and culture of Japan.

REFERENCES

Adams JC, Watt FM. 1993. Regulation of development and differentiation by the extracellular matrix. Development 117:1183–1198.

Cavaliere F, Florenzano F, Amadio S, Fusco FR, Viscomi MT, D'Ambrosi N, Vacca F, Sancesario G, Bernardi G, Molinari M, et al. 2003. Up-regulation of P2X2, P2X4 receptor and ischemic cell death: prevention by P2 antagonists. Neuroscience 120:85–98.

Farooque M, Zhang Y, Holtz A, Olsson Y. 1992. Exudation of fibronectin and albumin after spinal cord injury in rats. Acta Neuropathol (Berl) 84:613–620.

Hoke A, Silver J. 1996. Proteoglycans and other repulsive molecules in glial boundaries during development and regeneration of the nervous system. Prog Brain Res 108:149–163.

Hynes RO. 1992. Integrins: versatility, modulation, and signaling in cell adhesion. Cell 69:11–25.

Inoue K. 2002. Microglial activation by purines and pyrimidines. Glia 40:156–163.

Jiang B, Liou GI, Behzadian MA, Caldwell RB. 1994. Astrocytes modulate retinal vasculogenesis: effects on fibronectin expression. J Cell Sci 107:2499–2508.

Jones LS. 1996. Integrins: possible functions in the adult CNS. Trends Neurosci 19:68–72.

Krolo M, Vilovic K, Sapunar D, Vrdoljak E, Saraga-Babic M. 1998. Fibronectin expression in the developing human spinal cord, nerves, and ganglia. Croat Med J 39:386–391.

Le KT, Babinski K, Seguela P. 1998. Central P2X4 and P2X6 channel subunits coassemble into a novel heteromeric ATP receptor. J Neurosci 18:7152–7159.

Lefcort F, Venstrom K, McDonald JA, Reichardt LF. 1992. Regulation of expression of fibronectin and its receptor, alpha 5 beta 1, during development and regeneration of peripheral nerve. Development 116: 767–782.

Martini R. 1994. Expression and functional roles of neural cell surface molecules and extracellular matrix components during development and regeneration of peripheral nerves. J Neurocytol 23:1–28.

Matthiessen HP, Schmalenbach C, Muller HW. 1989. Astroglia-released neurite growth-inducing activity for embryonic hippocampal neurons is associated with laminin bound in a sulfated complex and free fibronectin. Glia 2:177–188.

Milner R, Campbell IL. 2002. Cytokines regulate microglial adhesion to laminin and astrocyte extracellular matrix via protein kinase C-dependent activation of the alpha6beta1 integrin. J Neurosci 22: 1562–1572.

Milner R, Campbell IL. 2003. The extracellular matrix and cytokines regulate microglial integrin expression and activation. J Immunol 170: 3850–3858.

Nag S, Picard P, Stewart DJ. 2001. Expression of nitric oxide synthases and nitrotyrosine during blood-brain barrier breakdown and repair after cold injury. Lab Invest 81:41–49.

Nakajima K, Shimojo M, Hamanoue M, Ishiura S, Sugita H, Kohsaka S. 1992. Identification of elastase as a secretory protease from cultured rat microglia. J Neurochem 58:1401–1408.

Nasu-Tada K, Koizumi S, Inoue K. 2005. Involvement of beta1 integrin in microglial chemotaxis and proliferation on fibronectin: different regulations by ADP through PKA. Glia 52:98–107.

Nourhaghighi N, Teichert-Kuliszewska K, Davis J, Stewart DJ, Nag S. 2003. Altered expression of angiopoietins during blood-brain barrier breakdown and angiogenesis. Lab Invest 83:1211–1222.

Pasinetti GM, Nichols NR, Tocco G, Morgan T, Laping N, Finch CE. 1993. Transforming growth factor beta 1 and fibronectin messenger RNA in rat brain: responses to injury and cell-type localization. Neuroscience 54:893–907.

Price J, Hynes RO. 1985. Astrocytes in culture synthesize and secrete a variant form of fibronectin. J Neurosci 5:2205–2211.

Raghow R. 1994. The role of extracellular matrix in postinflammatory wound healing and fibrosis. Faseb J 8:823–831.

Ralevic V, Burnstock G. 1998. Receptors for purines and pyrimidines. Pharmacol Rev 50:413–492.

Sakai T, Johnson KJ, Murozono M, Sakai K, Magnuson MA, Wieloch T, Cronberg T, Isshiki A, Erickson HP, Fassler R. 2001. Plasma fibronectin supports neuronal survival and reduces brain injury following transient focal cerebral ischemia but is not essential for skin-wound healing and hemostasis. Nat Med 7:324–330.

Sasaki Y, Hoshi M, Akazawa C, Nakamura Y, Tsuzuki H, Inoue K, Kohsaka S. 2003. Selective expression of Gi/o-coupled ATP receptor P2Y12 in microglia in rat brain. Glia 44:242–250.

Soto F, Garcia-Guzman M, Gomez-Hernandez JM, Hollmann M, Karschin C, Stuhmer W. 1996. P2X4: an ATP-activated ionotropic receptor cloned from rat brain. Proc Natl Acad Sci USA 93:3684–3688.

Thompson PN, Cho E, Blumenstock FA, Shah DM, Saba TM. 1992. Rebound elevation of fibronectin after tissue injury and ischemia: role of fibronectin synthesis. Am J Physiol 263:G437–G445.

Tom VJ, Doller CM, Malouf AT, Silver J. 2004. Astrocyte-associated fibronectin is critical for axonal regeneration in adult white matter. J Neurosci 24:9282–9290.

Tsuda M, Inoue K, Salter MW. 2005. Neuropathic pain and spinal microglia: a big problem from molecules in "small" glia. Trends Neurosci 28:101–107.

Tsuda M, Shigemoto-Mogami Y, Koizumi S, Mizokoshi A, Kohsaka S, Salter MW, Inoue K. 2003. P2X4 receptors induced in spinal microglia gate tactile allodynia after nerve injury. Nature 424:778–783.

Venstrom KA, Reichardt LF. 1993. Extracellular matrix. 2: Role of extracellular matrix molecules and their receptors in the nervous system. Faseb J 7:996–1003.

Vogelezang MG, Scherer SS, Fawcett JW, ffrench-Constant C. 1999. Regulation of fibronectin alternative splicing during peripheral nerve repair. J Neurosci Res 56:323–333.

Yeung D, Kharidia R, Brown SC, Gorecki DC. 2004. Enhanced expression of the P2X4 receptor in Duchenne muscular dystrophy correlates with macrophage invasion. Neurobiol Dis 15:212–220.

Zhang FL, Luo L, Gustafson E, Palmer K, Qiao X, Fan X, Yang S, Laz TM, Bayne M, Monsma F, Jr. 2002. P2Y(13): identification and characterization of a novel Galphai-coupled ADP receptor from human and mouse. J Pharmacol Exp Ther 301:705–713.

Purinergic Signalling (2005) 0: 1–8

Upregulation of P2Y2 receptors by retinoids in normal human epidermal keratinocytes

Kayoko Fujishita[1,2], Schuichi Koizumi[2] & Kazuhide Inoue[1,3]
[1]*Division of Biosignaling, National Institute of Health Science, 1-18-1 Kamiyoga, Setagaya, Tokyo, Japan;* [2]*Division of Pharmacology, National Institute of Health Science, 1-18-1 Kamiyoga, Setagaya, Tokyo, Japan;* [3]*Graduate School of Pharmaceutical Science, Kyusyu University, 3-1-1 Maidashi, Higashi, Fukuoka, Japan*

Received 17 February 2005; accepted in revised form 4 May 2005

Key words: ATP, P2Y2 receptors, retinoids, skin, transcription

Abstract

Retinoids, vitamin A derivatives, are important regulators of the growth and differentiation of skin cells. Although retinoids are therapeutically used for several skin ailments, little is known about their effects on P2 receptors, known to be involved in various functions in the skin. DNA array analysis showed that treatment of normal human epidermal keratinocytes (NHEKs) with all-*trans*-retinoic acid (ATRA), an agonist to RAR (retinoic acid receptor), enhanced the expression of mRNA for the P2Y2 receptor, a metabotropic P2 receptor that is known to be involved in the proliferation of the epidermis. The expression of other P2 receptors in NHEKs was not affected by ATRA. ATRA increased the mRNA for the P2Y2 receptor in a concentration-dependent fashion (1 nM to 1 μM). Am80, a synthesized agonist to RAR, showed a similar enhancement, whereas 9-*cis*-retinoic acid (9-*cis*RA), an agonist to RXR (retinoid X receptor), enhanced P2Y2 gene expression to a lesser extent. Ca^{2+} imaging analysis showed that ATRA also increased the function of P2Y2 receptors in NHEKs. Retinoids are known to enhance the turnover of the epidermis by increasing both proliferation and terminal differentiation. The DNA microarray analysis also revealed that ATRA upregulates various genes involved in the differentiation of NHEKs. Our present results suggest that retinoids, at least in part, exert their proliferative effects by upregulating P2Y2 receptors in NHEKs. This effect of retinoids may be closely related to their therapeutic effect against various ailments or aging events in skins such as over-keratinization, pigmentation and re-modeling.

Abbreviations: ATRA – all-trans retinoic acid; $[Ca^{2+}]i$ – intracellular calcium concentration; 9-cisRA – 9-cis retinoic acid; $InsP_3$ – inositol 1,4,5-trisphosphate; 2MeSADP – 2-methyl-thio-ADP; NHEKs – normal human epidermal kratinocytes; RAR – retinoic acid receptor; RXR – retinoid X receptor; UTP – uridine 5′-triphosphate

Introduction

The epidermis, the outermost part of the skin tissue, is a stratified squamous epithelium composed principally of keratinocytes with a highly dynamic structure [1]. Basal keratinocytes are located immediately above the basement membrane that separates the epidermal and dermal compartments. The basal layer is a proliferative layer from which keratinocytes withdraw from the cell cycle and commit to terminal differentiation. Differentiating cells migrate to the skin surface, going through suprabasal layers known as the spinous and granular layers. At the skin surface, dead and terminally-differentiated keratinocytes compose the stratum corneum, the so-called skin barrier. The skin covers most of the body and is exposed to multiple external stimuli such as dryness, chemicals, noxious heat, and UV light.

Endogenous chemical transmitters such as ATP, bradykinin, and histamine modulate skin physiology under normal conditions, after skin injury, and during inflammatory diseases and allergic reactions. Epidermal cells change the intracellular Ca^{2+} concentration ($[Ca^{2+}]i$) in response to various environmental stimuli [2–5]. The change in $[Ca^{2+}]i$ is an essential factor for the homeostasis of the skin epidermis and the regulation of the growth of epidermal keratinocytes [6–8]. Because of exposure to such stimuli, the skin causes an aberrant change in $[Ca^{2+}]i$ and often suffers aging damages such as over-keratinization, pigmentation and re-modeling (e.g., formation of wrinkles).

Vitamin A is known as one of the vital nutrients for the body. Retinyl esters and β-carotene from diet are converted

Correspondence to: Dr Kazuhide Inoue, PhD, Department of Molecular and System Pharmacology, Graduate School of Pharmaceutical Sciences, Kyushu University, Maidashi, Higashi, Fukuoka 812-8582, Japan. Tel: +81-92-642-4729; Fax: +81-92-642-4729; E-mail: inoue@phar.kyushu-u.ac.jp

DOI 10.1007/s11302-005-0373-7/PUSI2005-037; No. of Pages 8

to retinol and retinal and transported to the tissues by the circulation. They are then metabolized to retinoic acid (RA), a biologically active metabolite of retinoids [9]. Retinoids have been used clinically to prevent aging events or other disorders in the skin. RA works through gene activation as a ligand of the nuclear receptors for retinoic acid (RARα, β and γ), and the retinoid X receptors (RXRα, β and γ) [10, 11]. RARs bind all-*trans*-RA (ATRA), whereas RXRs interact exclusively with 9-*cis*RA stereo-isomers. Retinoid signals are believed to be transduced by RAR–RXR heterodimers [11], but RXRs have also been shown to be heterodimeric partners of a number of other members of the nuclear receptor superfamily (e.g., vitamin D receptors and peroxisome proliferators) [12]. The epidermis expresses RXRα, RXRβ, RARα and RARγ. RXRα and RARγ are dominant in their expression [9]. Although retinoids acting on these nuclear receptors regulate both epidermal proliferation and differentiation [13–15], little is known about the molecular cascades linking the retinoid receptors to cell growth/differentiation.

Adenosine 5′-triphosphate (ATP) is now recognized as an important extracellular molecule that mediates cell-to-cell communication via ATP receptors, P2 receptors. P2 receptors are classified into two subfamilies; the ligand-gated channel P2X receptors (P2X1-7) and the G protein-coupled P2Y receptors (P2Y1,2,4,6,11-14). P2 receptors are distributed in almost all tissues in the body including the skin. Exogenously applied ATP causes an increase in $[Ca^{2+}]i$ in human epidermal keratinocytes [2]. Cultured human keratinocytes can release ATP in response to mechanical stimulation [16] or even spontaneously [3]. Skin cells express P2 receptors, especially P2X5, P2X7, P2Y1 and P2Y2 receptors, each of which is expressed in a spatially distinct zone of the epidermis and has distinct functions in epidermal cell growth and/or differentiation [17]. Recently, we have reported that mechanical stimulation of single normal human epidermal keratinocytes (NHEKs) produces a propagating Ca^{2+} wave that is mediated by extracellular ATP and the activation of P2Y2 receptors [16]. The P2Y2 receptor has been found to be a critical molecule that regulates the proliferation of the basal layer of the epidermis [17]. These findings suggest that intracellular signals mediated by P2Y2 receptors are closely involved in various epidermal functions. We hypothesize that regulation of P2Y2 receptor-mediated signals could lead to therapeutic effects against several ailments or aging events in skin such as over-keratinization, pigmentation and re-modeling.

In the present study, we report that the treatment of cells with retinoids selectively upregulated the mRNA and function of P2Y2 receptors in NHEKs. We also demonstrate that the upregulation is mainly mediated by RAR, presumably RARα. The RARα agonist ATRA mimics an increases in P2Y2 receptors without increasing other P2 receptors in NHEKs. Our present findings suggest that retinoids might at least in part exert their therapeutic effects by controlling ATP/P2Y2 receptor-mediated signals.

Materials and methods

Chemicals

All-*trans* retinoic acid (ATRA), 9-*cis* retinoic acid (9-*cis*RA) and uridine 5′-triphosphate (UTP) were purchased from Sigma Chemical Co. (St. Louis, MO). Am80 was a kind gift from Prof. Kagechika (Tokyo Univ.) [18]. Retinoids and Am80 were dissolved in ethanol and stored at −30 °C.

Cells and cell culture

Normal human epidermal keratinocytes (NHEKs) were obtained as cyropreserved first-passage cells from neonatal foreskins (Kurabo, Osaka, Japan). Cells were cultured in serum-free keratinocyte growth medium, Humedia-KB2 (Kurabo, Osaka, Japan) supplemented with bovine pituitary extract (0.4% v/v), human recombinant epidermal growth factor (0.1 ng/ml), insulin (10 μg/ml), hydrocortisone (0.5 μg/ml), gentamicin (50 μg/ml) and amphotericin-B (50 ng/ml). The medium was replaced every 2–3 days. In the case of retinoid treatment, the normal culture medium was replaced with the non-supplemented Humedia-KB2 about 24 h before the retinoid treatment in order to remove possible effects from the medium. For Ca^{2+} imaging experiments, cells were plated on collagen-coated coverslips.

Total RNA preparation

NHEKs were prepared in collagen-coated 60 mm dishes (1.5×10^5 cells/dish). After washing the cells twice with PBS, total RNA was prepared with an RNeasy Mini total RNA Preparation Kit (Qiagen GmbH, Hilden, Germany) according to the manufacturer's instructions.

Quantitative RT-PCR of P2 receptors

RT-PCR amplifications were performed using Taqman One-step RT-PCR Master Mix Reagents, and 200 nM of each P2 receptor specific primer and 100 nM of Taqman probe. Using Primer Express computer software, (Applied Biosystems Japan Ltd., Tokyo, Japan), clone-specific primers were designed to recognize human P2Y1 (Taqman Probe, 5′-tcagaccccagcaatgtgtgctttca-3′; forward, 5′-gagggcccggcttgatt-3′; reverse, 5′-atacgtggcataaaccctgtca-3′), P2Y2 (Taqman probe, 5′-aacctttactgcagcatcctcttcctcacc-3′; forward, 5′-tggtgcgcttcctcttctaca-3′; reverse, 5′-accggtgca-cgctgatg-3′), and P2Y11 (Taqman probe, 5′-cgacgacaaactcagtgggttccagg-3′; forward, 5′-ctgccctgccaacttcttg-3′; reverse, 5′-accagtatgggccacaggaa-3′) receptors mRNA sequences. All primers had similar melting temperatures for running the same cycling program for all samples. RT-PCR was done by 30 min reverse transcription at 48 °C, 10 min AmpliTaq Gold activation at 95 °C, then 15 s denaturation at 95 °C, 1 min annealing and elongation at 60 °C for 40 cycles in a PRISM7700 (Applied Biosystems Japan Ltd). To exclude

the contamination of unspecific PCR products such as primer dimmers, melting curve analysis was applied to all final PCR products after the cycling protocol. Primers for glyceraldehyde 3-phosphate dehydrogenase (GAPDH, Applied Biosystems Japan Ltd) was used for normalization.

DNA micro-array analysis

Converting total RNA to the targets for Affymetrix GeneChip DNA microarray hybridization was done according to the manufacturer's instructions. The targets were hybridized to human genome U95A GeneChip DNA microarray (Affymetrix, Santa Clara, CA, USA) for 16–24 h at 45 °C. After the hybridization, the DNA microarrays were washed and stained on Fluidics Station (Affymetrix) according to the protocol provided by Affymetrix. Then, the DNA microarrays were scanned, and the images obtained were analyzed by Microarray Suite Expression Analysis Software (version 4.0; Affymetrix). The DNA microarray analysis data was obtained from six independent samples ($n = 6$).

Ca^{2+} imaging in single NHEKs

NHEKs were cultured in collagen-coated glass coverslips at density of 1×10^5 cells/ml. Changes in the intracellular calcium concentration ($[Ca^{2+}]i$) in single cells were measured by the fura-2 method as described by Grynkiewicz et al. [19] with minor modifications [20]. In brief, the culture medium of cells grown on a coverslip was replaced with balanced salt solution (BSS) of the following composition (mM): NaCl 150, KCl 5.0, $CaCl_2$ 1.8, $MgCl_2$ 1.2, *N*-2-hydroxyethylpiperazine-*N'*-2-ethanesulfonic acid (HEPES) 25, and D-glucose 10 (pH = 7.4). The cells were loaded with 5 μM fura-2 acetoxymethylester (fura-2 AM) (Molecular Probes Inc., Eugene) at room temperature (20–22 °C) in BSS for 45 min, followed by BSS and a further 15 min incubation to allow de-esterification of the loaded dye. The coverslips were mounted on an inverted epifluorescence microscope (TE-2000-U, Nikon, Tokyo, Japan). Fluorescent images were obtained by alternate excitation at 340 (F340) and 380 (F380) nm. The emission signal at 510 nm was collected by a charge-coupled device camera (C-6790, Hamamatsu Photonics, Hamamatsu, Japan) coupled with an image intensifier (GaAsP, C8600-03, Hamamatsu Photonics), and digitized signals were stored and processed using an image processing system (Aquacosmos, Hamamatsu Photonics, Hamamatsu, Japan). Drugs were dissolved in BSS and applied by superfusion.

Detection of ATP release

NHEKs were prepared in collagen-coated 22 × 40 mm chamber glasses at a density of 1×10^5 cells/ml. After superfusion with BSS for 5 min, the cell chamber was filled with a luciferin–luciferase reagent (ATP bioluminescence assay kit CLS, Roche Diagnostics GmbH, Mannheim, Germany). ATP bioluminescence was detected and visualized with a VIM camera (C2400-35, Hamamatsu Photonics, Hamamatsu, Japan) using an integration time of 10 s. The absolute ATP concentration was estimated by using standard ATP solution (Roche Diagnostics GmbH). Data were imaged with Aquacosmos software (Hamamatsu Photonics) and analyzed with NIH-image 1.61 software (Apple computer, Inc., USA). For mechanical stimulation, a single NHEK in the center of the microscopic field was probed with a glass micropipette using a micromanipulator (Narishige, Tokyo, Japan). Under visible light, the tip of the micropipette was positioned approx. 2 μm over the cell to be stimulated. When sampling, the micropipette was rapidly lowered by approx. 2 μm and then rapidly returned to its original position. If the stimulated cell showed any sign of damage (abnormal morphology), the experiment was eliminated.

Statistics

Experimental results are expressed as mean ± SEM Statistical differences between two groups were determined by Student's *t*-test (including the DNA microarray experiments). The multiple linear regression was used to analyze the effect of various concentrations of retinoids on P2Y2 receptor expression. The percentage of the P2Y2 receptor mRNA expression was chosen as outcome variable, and the exposure time of retinoids at each concentration was dummy coded and used as predictor variables.

Results

Retinoids upregulate mRNAs for P2Y2 receptors in NHEKs

The skin expresses multiple P2 receptors. We previously showed that the expression of P2Y1, P2Y2 and P2Y11 is relatively higher in NHEKs [16]. Firstly, we examined the changes in the mRNAs for the P2 receptors induced by retinoids in NHEKs using DNA array analysis. Unfortunately, the DNA microarray we used (U95A GeneChip DNA microarray) does not contain all cloned *P2* receptor genes (for example, P2Y11 receptors) but it contains *P2Y1*, *P2Y2*, *P2Y6*, *P2X1*, *P2X3*, *P2X4*, *P2X5* and *P2X7* receptor genes. Treatment of NHEKs with 0.1 μM all-*trans* retinoic acid (ATRA) for 6 h caused a drastic increase in the mRNA for P2Y2 receptor (304.1 ± 38.1% of control, $n = 3$). Interestingly, ATRA did not affect the expression of any other P2 receptors included in U95A GeneChip (Table 1), suggesting that ATRA selectively upregulates P2Y2 receptors in NHEKs. This result was confirmed quantitatively using real-time RT-PCR (Figure 1). Treatment of NHEKs with ATRA induced a similar increase in the mRNA for P2Y2 receptors (264.4 ± 59.1% of control, $n = 3$) but not for other P2 receptors such as P2Y1 and P2Y11 (P2Y1, 67.5 ± 6.67, $n = 3$; P2Y11, 70.0 ± 11.7% of control, $n = 3$).

t1.1 *Table 1.* ATRA-induced changes in expression pattern of P2 receptors in NHEKs.

t1.2 Gene title	Abbreviations	Percentage of control (%)	Statistics
t1.3 Purinergic receptor P2X, ligand-gated ion channel, 1	P2RX1	94.9 ± 8.5	
t1.4 Purinergic receptor P2X-like 1, orphan receptor	P2RXL1	28.2 ± 40.1	
t1.5 Purinergic receptor P2X, ligand-gated ion channel, 3	P2RX3	138.9 ± 36.7	
t1.6 Purinergic receptor P2X, ligand-gated ion channel, 4	P2RX4	88.9 ± 23.4	
t1.7 Purinergic receptor P2X, ligand-gated ion channel, 5	P2RX5	184.5 ± 41.7	
t1.8 Purinergic receptor P2X, ligand-gated ion channel, 7	P2RX7	78.1 ± 17.4	
t1.9 Purinergic receptor P2Y, G-protein coupled, 1	P2RY1	58.6 ± 18.7	
t1.10 Purinergic receptor P2Y, G-protein coupled, 2	P2RY2	304.1 ± 38.1	**
t1.11 Pyrimidinergic receptor P2Y, G-protein coupled, 6	P2RY6	76.4 ± 9.7	

t1.12 Cells were incubated with 0.1 μM ATRA for 6 h. The expression levels of each gene are shown as the average of triplicate microarray measurements. Asterisks show significant difference from control groups (**$P < 0.01$). Data were normalized by the signals in control (0.5% ethanol).

We next investigated the time-course and concentration dependency of changes in the mRNA expression for P2Y2 receptors induced by ATRA, its stereo-isomer 9-*cis* retinoic acid (9-*cis*RA) and the synthetic RAR agonist Am80. All these retinoids tested caused significant and drastic increases in the mRNA expression in a concentration- and incubation time-dependent manner (Figure 2). After treatment with 1 μM ATRA and Am80 for 24 h, the expression level reached to 768.4 ± 458.1 and 862.2 ± 24.7% of control, respectively (Figure 2A, B). 9-*cis*RA, an agonist to RXRs and possibly to RARs, showed a moderate but significant rise in P2Y2 receptor mRNA in NHEKs (Figure 2C). These results suggest that the upregulation of P2Y2 receptors by retinoids would be mainly mediated by RARs in NHEKs.

Enhancement by ATRA of the UTP-evoked increase in $[Ca^{2+}]i$ in NHEKs

We next investigated whether ATRA increases the function of P2Y receptors in NHEKs. Activation of phospholipase C (PLC)-linked P2Y2 receptors in NHEKs results in an increase in $[Ca^{2+}]i$ via inositol-1,4,5-trisphosphate ($InsP_3$)-mediated Ca^{2+} release from stores [21]. We therefore investigated the effect of ATRA on the increase in $[Ca^{2+}]i$ evoked by UTP, an agonist to P2Y2 receptors, in NHEKs. The cells were stimulated with 0.1 μM ATRA or Am80 for 6 h, and then were incubated with normal culture medium for an additional 18 h. UTP (100 μM) produced an increases in $[Ca^{2+}]i$ in NHEKs that were significantly enhanced by the ATRA- and Am80-treatment (133.2 ± 4.1 and 127.8 ± 6.3% of control, respectively (Figure 3B)). Similar enhancement of Ca^{2+} responses to UTP in retinoids-treated and -untreated cells was observed even in the absence of extracellular Ca^{2+} (Figure 3A). These results suggest that ATRA and Am80 upregulates functional P2Y2 receptor in NHEKs without changing the nature of Ca^{2+} signals.

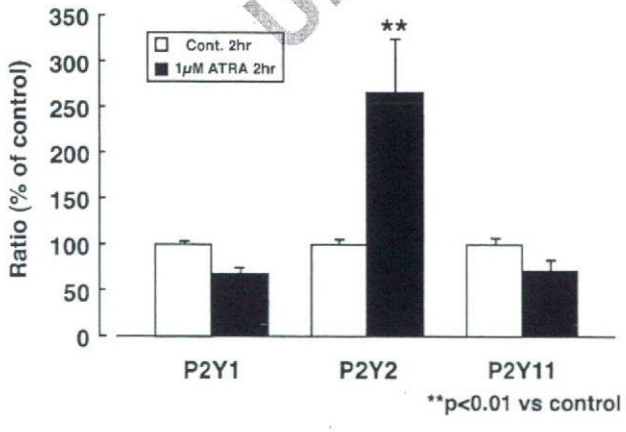

Figure 1. Changes in mRNA expression for P2Y receptors induced by ATRA in NHEKs. Diagram shows the percentage of the quantity after amplification by real-time RT-PCR for P2Y1, P2Y2 and P2Y11 receptor mRNAs extracted from NHEKs treated with 1 μM ATRA for 2 h. Asterisks show significant difference from control groups (*white columns*, **$P < 0.01$). mRNAs of P2Y2 receptors were increased by more than two-fold vs. control. Data were obtained from at least three independent experiments.

ATRA decreases spontaneous ATP release from NHEKs

NHEKs release ATP in response to mechanical stimulation [16] or even spontaneously [3]. Endogenously released ATP and activation of P2Y2 receptors form propagating Ca^{2+} waves in NHEKs [16]. We thus investigated whether ATRA affects the release of ATP from NHEKs. Similarly as in Figure 3, the cells were treated with 0.1 μM ATRA for 6 h, and then incubated for another 18 h with normal culture medium. The cells were bathed in solution containing luciferin–luciferase reagent and photons were counted every 10 s prior to and after mechanical stimulation of the NHEKs in a dark box. The left panels in Figure 4Aa & a′ show phase contrast images of microscopic fields, and the remaining panels (b–e & b′–e′) in Figure 4A show bioluminescence images 10 s before (b & b′) and 10 (c & c′), 20 (d & d′), 30 s (e & e′) after mechanical stimulation in the same field. ATP was released and diffused from the stimulated site in both cultures. We found that the release of ATP peaked around 10 s after mechanical stimulation, and then gradually decreased to the pre-stimulated level in 60 s. The release of ATP at 10 s after mechanical stimulation in ATRA-treated cells is higher than that in control cells (Figure 4A c vs. c′). The photons derived from ATP with and without mechanical stimulation were accumulated for 60 s in both ATRA-treated and -untreated cells and

compared, which was summarized in B. For photon counting, we defined a rectangle (50 μms squares) at the center of the stimulated site, and then measured the averaged photon intensity within the squares (see Figure 4Aa & a′ white squares), which was then converted to the absolute ATP concentration using a standard ATP-photon-intensity curve. Mechanical stimulation produced a significant rise in the extracellular ATP concentration in ATRA-treated and control NHEKs (Figure 4B). The extracellular ATP concentrations 60 s after stimulation in ATRA-treated and control NHEKs were 7.30 ± 1.31 (n = 17) and 5.28 ± 0.94 (n = 14) μM, respectively ($P < 0.05$). However, the basal ATP concentration in ATRA-treated NHEKs was significantly lower than that in control cells (Figure 4B, 3.09 ± 0.88 (n = 17) vs. 1.40 ± 0.16 (n = 14) μM, $P < 0.05$).

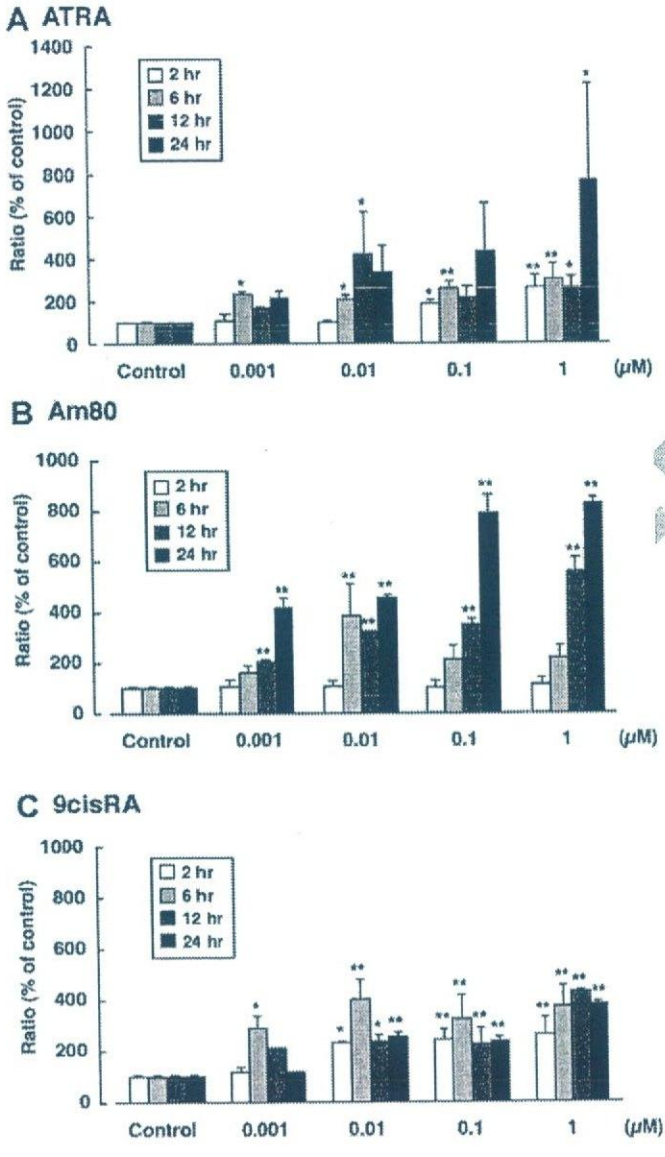

Figure 2. Time- and concentration-dependency of three different retinoids-induced changes in mRNAs in NHEKs. Diagram shows the quantity of P2Y2 mRNAs detected by real-time RT-PCR after treatment with 0.001–1 μM ATRA (A), Am80 (B) and 9-*cis*RA (C) for 2–24 h. The P2Y2 mRNA levels in cells treated with various concentrations of retinoids were normalized by those in retinoids-untreated control cells at each incubation period (2, 6, 12 and 24 h), and expressed as "percentage (%) of control." All these retinoids, and especially Am80, caused a linear increase in P2Y2 mRNAs in a concentration- and time-dependent fashion. *Asterisks* show significant difference in the P2Y2 mRNA levels from control groups (*$P < 0.05$; **$P < 0.01$). Data were obtained from at least three independent experiments.

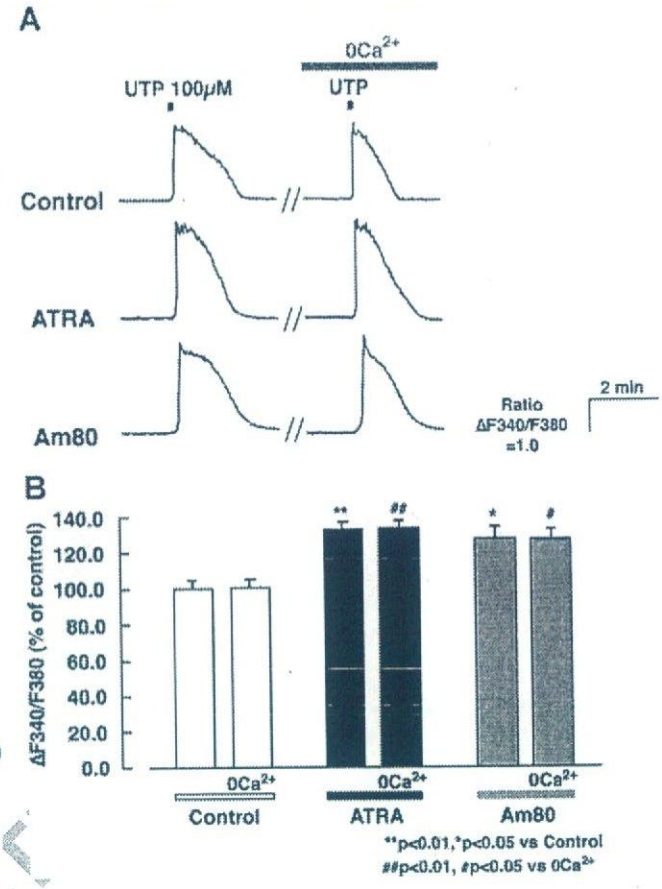

Figure 3. Enhancement by ATRA and Am80 of P2Y2 receptor-mediated increase in $[Ca^{2+}]i$ in NHEKs. A. Typical traces of the UTP-evoked changes in $[Ca^{2+}]i$ in NHEKs. NHEKs were incubated with 0.1 μM ATRA (*middle*) or Am80 (*bottom*) for 6 h, incubated with normal culture medium for another 18 h, and then the fura-2 based $[Ca^{2+}]i$ measurement was performed. UTP (100 μM) was applied to cells for 10 s and the increase in the ΔF340/F380 ratio was calculated (n = 110–125). After the initial UTP-application, the extracellular Ca^{2+} was removed (0 Ca^{2+}), and the second UTP was applied to the cells in the absence of extracellular Ca^{2+}. Effect of ATRA and Am80 on the UTP-evoked elevation in $[Ca^{2+}]i$ in NHEKs in the presence and absence of extracellular Ca^{2+} was summarized in B. *Asterisks* show significant difference from control (without retinoids) (*$P < 0.05$; **$P < 0.01$).

Discussion

In the present study, we demonstrated that ATRA and Am80, a synthesized agonist to RARs, selectively increased the expression of P2Y2 receptors in cultured NHEKs. P2Y2 receptors are relatively localized at the proliferative basal layer of keratinocytes [17], and activation of P2Y2 receptors results in proliferation of the epidermis *in vivo* [17] and *in vitro* [3]. Retinoids are known to induce both epidermal proliferation and differ-

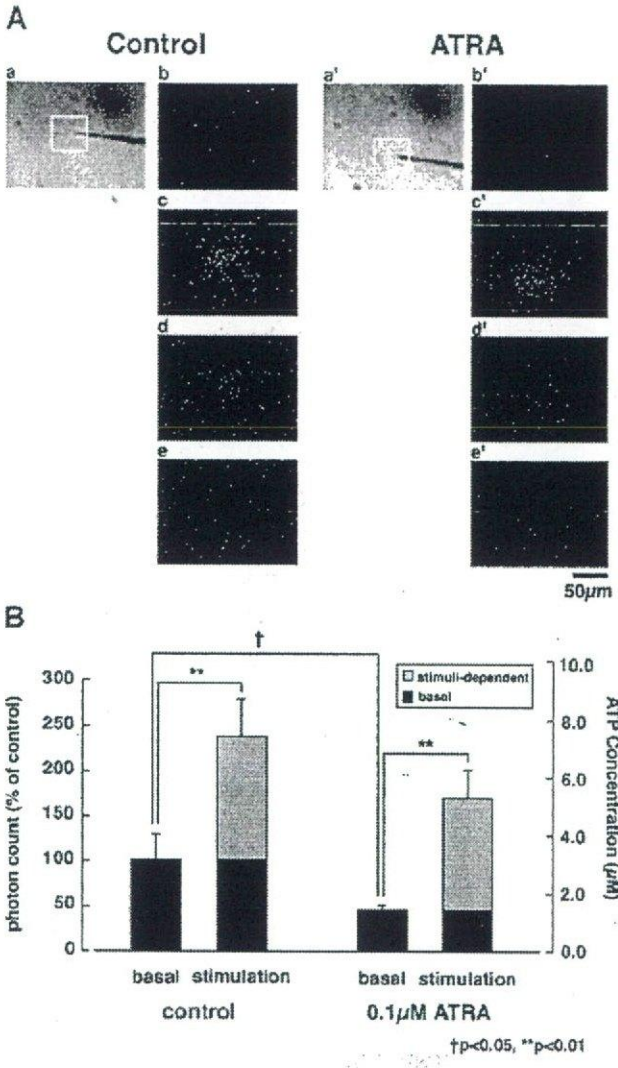

Figure 4. Visualization of release of ATP from NHEKs. The image panels in A show ATP-derived photons (*white dots*) in a field of ATRA-treated (*right*) and -untreated control NHEKs (*left*). NHEKs were incubated with 0.1 μM ATRA for 6 h. Cells were bathed in luciferin–luciferase reagent and the bioluminescence signals were obtained with a VIM camera (see Materials and methods Section) with an exposure time of 10 s. Sequential images show the ATP-derived photon-signals before (−10 s; b & b′) and 10 (c & c′), 20 (d & d′) and 30 s (e & e′) after mechanical stimulation. The positions of the pipettes are shown in phase-contrast images of NHEKs (a & a′). In B, the accumulative photon intensity in 60 s was converted to the absolute extracellular ATP concentration using a standard ATP-photon intensity relationship curve determined with an ATP standard solution (control, $n = 17$; ATRA-treated, $n = 14$). Photons within 50 μms squares around the stimulated site (shown as white squares in a & a′ panels in A) were calculated. Asterisks show significant difference from basal groups ($^{**}P < 0.01$) and dagger shows significant difference from control basal groups ($^{\dagger}P < 0.05$).

entiation. These findings strongly suggest that upregulation of P2Y2 receptors by retinoids may be the mechanism by which retinoids induce the cell growth of proliferative basal keratinocytes.

Ever since the discovery of retinoic acid, there has been growing interest in retinoid-induced pleiotropic effects [11]. With regard to the skin, retinoids have been used clinically for various skin disorders or problems such as psoriasis [25], wrinkles [26],[23] acne [27][21] and cancer [28–30]. Although retinoids can act on organs other than the epidermis and reveal their therapeutic effects, for example, facilitation of collagen formation in the dermis and inhibition of sebaceous gland activities, they directly act on the epidermis itself and regulate both its proliferation and differentiation [13–15]. The epidermis expresses RARs and RXRs, especially RARγ and RXRα [9]. Activation of RARs causes keratinocytic differentiation and hyperproliferation [31][29] [14]. RXRα are involved in retinoid-induced cell proliferation in adult mouse skin [32],[20] and RARγ/RXRα heterodimers in suprabasal keratinocytes are required for retinoid-induced epidermal hyperplasia [15]. In the present study, we showed that ATRA and Am80 dramatically and selectively increased the expression of P2Y2 receptors. Subcutaneous injection of UTP, an agonist to P2Y2 receptors, generates epidermal hyperplasia that results from hyperproliferation of basal keratinocytes *in vivo* [17]. Incubation of cultured keratinocytes with UTP causes epidermal proliferation *in vitro* [3]. These findings suggest that P2Y2 receptors in basal keratinocytes may be an important target for retinoid-induced proliferation, i.e., retinoids acting mainly on RARs, presumably RARγ, in the epidermis upregulate the expression and function of P2Y2 receptors, thereby leading to the proliferation of basal keratinocytes. Xiao et al. (1999) have already shown that activation of RARγ/RXRα heterodimers in epidermis resulted in the upregulation of heparin-binding epidermal growth factor (HB-EGF), by which retinoid induces the cell growth of basal keratinocytes [14]. However, the production of HB-EGF occurs not in basal layer but in differentiated suprabasal cells which in turn stimulate basal keratinocytes to proliferate in a paracrine manner. We used cultured NHEKs and demonstrated that both ATRA and Am80 selectively upregulated *P2Y2* receptor genes and their functions. Keratinocytes cultured *in vitro* are considered to be similar to basal layer keratinocytes *in vivo* based on their ability to proliferate and express basal cell-specific genes such as keratin-5 or keratin-14 [33].[30] P2Y2 receptors are mainly localized in the proliferative basal layer of keratinocytes *in situ* [17]. Thus, in addition to differentiated suprabasal cells [14], retinoids seem to affect the function of basal keratinocytes directly to cause cell growth. NHEKs release ATP in response to mechanical stimulation, and retinoids had no significant effect on the evoked release of ATP (Figure 4). It is therefore suggested that ATP released from the basal cell layer and acting on P2Y2 receptors could function in an autocrine manner to control the proliferation in basal keratinocytes. Retinoids may cause proliferation by facilitating the ATP/P2Y2 autocrine signals. Although retinoids had no significant effect on the release of ATP in response to mechanical stimulation, they reduced the basal ATP release in NHEKs (Figure 4B). This complexity in the ATP release in NHEKs might explain the mixed and multiple effects of retinoids.

Basal keratinocytes also express P2Y1 receptors *in situ* [17]. However, the effect of the P2Y1 agonists 2methylthio-ADP (2MeSADP) on epidermal proliferation *in vivo* is

much weaker than that of UTP, suggesting that P2Y2 receptors have a more significant role in the proliferation [17]. P2Y1 and P2Y2 receptors share Gq/11-coupled intracellular signal cascades. Activation of both receptor results in inositol 1,4,5-trisphosphate ($InsP_3$) production, leading to Ca^{2+} mobilization from the store [34–36]. In addition, activation of both receptors also induces ERK1/2 MAPkinase cascades in some cells such as astrocytes [37, 38]. However, P2Y2 receptors seem to be much more closely related to proliferation of the epidermis. This discrepancy may be explained by the lower expression level of P2Y1 receptors in basal keratinocytes. In fact, the P2Y1 receptor agonist 2meSADP caused only a slight increase in $[Ca^{2+}]i$ in cultured NHEKs [16], though quantitative analysis of the expression levels and localization of both receptors *in situ* are required to clarify this issue. In any case, retinoids upregulated the P2Y2 receptor but not P2Y1 receptor expression in NHEKs (Table 1 and Figure 1). The published sequence of the human *P2Y2* receptor gene promoter shows that the P2Y2 receptor has putative RAREs in the upstream promoter region (data not shown), which may also support that *P2Y2* receptors are a likely target gene for retinoids.

In summary, we demonstrated that retinoids upregulate P2Y2 receptors via mainly RAR in NEHKs. Judging from the well-known finding that activation of P2Y2 receptors regulates the proliferation of the epidermis, retinoids may exert their therapeutic effects through the upregulation of P2Y2 receptors in the skin.

Acknowledgements

We thank Dr Seiichi Ishida for useful advice concerning DNA array analysis, Dr Kaori Inoue for critical comments and Dr Yasuo Ohno for continuous encouragement. This work was supported by the Organization for Pharmaceutical Safety and Research (Medical Frontier Project; MF-16), The Health Science Foundation in Japan and Shiseido Research Center (Yokohama, Japan).

References

1. Fuchs E, Keith R. Porter lecture, 1996. Of mice and men: Genetic disorders of the cytoskeleton. Mol Biol Cell 1997; 8: 189–203.
2. Pillai S, Bikle DD. Adenosine triphosphate stimulates phosphoinositide metabolism, mobilizes intracellular calcium, and inhibits terminal differentiation of human epidermal keratinocytes. J Clin Invest 1992; 90: 42–51.
3. Dixon CJ, Bowler WB, Littlewood-Evans A et al. Regulation of epidermal homeostasis through P2Y2 receptors. Br J Pharmacol 1999; 127: 1680–6.
4. Genever PG, Maxfield SJ, Kennovin GD et al. Evidence for a novel glutamate-mediated signaling pathway in keratinocytes. J Invest Dermatol 1999; 112: 337–42.
5. Stoebner PE, Carayon P, Penarier G et al. The expression of peripheral benzodiazepine receptors in human skin: The relationship with epidermal cell differentiation. Br J Dermatol 1999; 140: 1010–6.
6. Tu CL, Chang W, Bikle DD. The extracellular calcium-sensing receptor is required for calcium-induced differentiation in human keratinocytes. J Biol Chem 2001; 276: 41079–85.
7. Elias PM, Ahn SK, Denda M et al. Modulations in epidermal calcium regulate the expression of differentiation-specific markers. J Invest Dermatol 2002; 119: 1128–36.
8. Komuves L, Oda Y, Tu CL et al. Epidermal expression of the full-length extracellular calcium-sensing receptor is required for normal keratinocyte differentiation. J Cell Physiol 2002; 192: 45–54.
9. Fisher GJ, Voorhees JJ. Molecular mechanisms of retinoid actions in skin. Faseb J 1996; 10: 1002–13.
10. Sucov HM, Evans RM. Retinoic acid and retinoic acid receptors in development. Mol Neurobiol 1995; 10: 169–84.
11. Chambon P. A decade of molecular biology of retinoic acid receptors. Faseb J 1996; 10: 940–54.
12. Giguere V. Orphan nuclear receptors: From gene to function. Endocr Rev 1999; 20: 689–725.
13. Saitou M, Sugai S, Tanaka T et al. Inhibition of skin development by targeted expression of a dominant-negative retinoic acid receptor. Nature 1995; 374: 159–62.
14. Xiao JH, Feng X, Di W et al. Identification of heparin-binding EGF-like growth factor as a target in intercellular regulation of epidermal basal cell growth by suprabasal retinoic acid receptors. Embo J 1999; 18: 1539–48.
15. Chapellier B, Mark M, Messaddeq N et al. Physiological and retinoid-induced proliferations of epidermis basal keratinocytes are differently controlled. Embo J 2002; 21: 3402–13.
16. Koizumi S, Fujishita K, Inoue K et al. Ca^{2+} waves in keratinocytes are transmitted to sensory neurons: The involvement of extracellular ATP and P2Y2 receptor activation. Biochem J 2004; 380: 329–38.
17. Greig AV, Linge C, Terenghi G et al. Purinergic receptors are part of a functional signaling system for proliferation and differentiation of human epidermal keratinocytes. J Invest Dermatol 2003; 120: 1007–15.
18. Kagechika H, Kawachi E, Hashimoto Y et al. Retinobenzoic acids: 2. Structure–activity relationships of chalcone-4-carboxylic acids and flavone-4′-carboxylic acids. J Med Chem 1989; 32: 834–40.
19. Grynkiewicz G, Poenie M, Tsien RY. A new generation of Ca^{2+} indicators with greatly improved fluorescence properties. J Biol Chem 1985; 260: 3440–50.
20. Koizumi S, Rosa P, Willars GB et al. Mechanisms underlying the neuronal calcium sensor-1-evoked enhancement of exocytosis in PC12 cells. J Biol Chem 2002; 277: 30315–24.
21. Koizumi S, Fujishita K, Tsuda M et al. Dynamic inhibition of excitatory synaptic transmission by astrocyte-derived ATP in hippocampal cultures. Proc Natl Acad Sci USA 2003; 100: 11023–8.
22. Steinert PM. The complexity and redundancy of epithelial barrier function. J Cell Biol 2000; 151: F5–8.
23. Ruhrberg C, Hajibagheri MA, Simon M et al. Envoplakin, a novel precursor of the cornified envelope that has homology to desmoplakin. J Cell Biol 1996; 134: 715–29.
24. Ruhrberg C, Hajibagheri MA, Parry DA et al. Periplakin, a novel component of cornified envelopes and desmosomes that belongs to the plakin family and forms complexes with envoplakin. J Cell Biol 1997; 139: 1835–49.
25. Gollnick HP, Dummler U. Retinoids. Clin Dermatol 1997; 15: 799–810.
26. Griffiths CE, Russman AN, Majmudar G et al. Restoration of collagen formation in photodamaged human skin by tretinoin (retinoic acid). N Engl J Med 1993; 329: 530–5.
27. Geiger JM. Retinoids and sebaceous gland activity. Dermatology 1995; 191: 305–10.
28. Lotan R. Retinoids in cancer chemoprevention. Faseb J 1996; 10: 1031–9.
29. Hansen LA, Sigman CC, Andreola F et al. Retinoids in chemoprevention and differentiation therapy. Carcinogenesis 2000; 21: 1271–9.
30. Verma AK. Retinoids in chemoprevention of cancer. J Biol Regul Homeost Agents 2003; 17: 92–7.
31. Imakado S, Bickenbach JR, Bundman DS et al. Targeting expression

of a dominant-negative retinoic acid receptor mutant in the epidermis of transgenic mice results in loss of barrier function. Genes Dev 1995; 9: 317–29.

32. Feng X, Peng ZH, Di W et al. Suprabasal expression of a dominant-negative RXR alpha mutant in transgenic mouse epidermis impairs regulation of gene transcription and basal keratinocyte proliferation by RAR-selective retinoids. Genes Dev 1997; 11: 59–71.

33. Sinha S, Degenstein L, Copenhaver C et al. Defining the regulatory factors required for epidermal gene expression. Mol Cell Biol 2000; 20: 2543–55.

34. Schachter JB, Li Q, Boyer JL et al. Second messenger cascade specificity and pharmacological selectivity of the human P2Y1-purinoceptor. Br J Pharmacol 1996; 118: 167–73.

35. Hechler B, Vigne P, Leon C et al. ATP derivatives are antagonists of the P2Y1 receptor: Similarities to the platelet ADP receptor. Mol Pharmacol 1998; 53: 727–33.

36. Parr CE, Sullivan DM, Paradiso AM et al. Cloning and expression of a human P2U nucleotide receptor, a target for cystic fibrosis pharmacotherapy. Proc Natl Acad Sci USA 1994; 91: 3275–9.

37. Neary JT, Kang Y, Willoughby KA et al. Activation of extracellular signal-regulated kinase by stretch-induced injury in astrocytes involves extracellular ATP and P2 purinergic receptors. J Neurosci 2003; 23: 2348–56.

38. Ahmad S, Ahmad A, Ghosh M et al. Extracellular ATP-mediated signaling for survival in hyperoxia-induced oxidative stress. J Biol Chem 2004; 279: 16317–25.

J Pharmacol Sci 98, 323 – 326 (2005)

Journal of Pharmacological Sciences

Short Communication

Forced Exercise-Induced Flushing of Tail Skin in Ovariectomized Mice, as a New Experimental Model of Menopausal Hot Flushes

Hideki Shuto[1], Atsushi Yamauchi[1], Munehiko Ikeda[1], Yoshio Sohda[1], Ayako Koga[1], Kohji Tominaga[1], Takashi Egawa[1], and Yasufumi Kataoka[1,*]

[1]*Department of Pharmaceutical Care and Health Sciences, Faculty of Pharmaceutical Sciences, Fukuoka University, 8-19-1 Nanakuma, Jonan-ku, Fukuoka 814-0180, Japan*

J Pharmacol Sci 98, 323 – 326 (2005)

Journal of Pharmacological Sciences

Short Communication

Forced Exercise-Induced Flushing of Tail Skin in Ovariectomized Mice, as a New Experimental Model of Menopausal Hot Flushes

Hideki Shuto[1], Atsushi Yamauchi[1], Munehiko Ikeda[1], Yoshio Sohda[1], Ayako Koga[1], Kohji Tominaga[1], Takashi Egawa[1], and Yasufumi Kataoka[1,*]

[1]*Department of Pharmaceutical Care and Health Sciences, Faculty of Pharmaceutical Sciences, Fukuoka University, 8-19-1 Nanakuma, Jonan-ku, Fukuoka 814-0180, Japan*

Received February 21, 2005; Accepted May 12, 2005

Abstract. Hot flushes are the most common complaint of menopausal women. In the present study, a new animal model of hot flushes was established. Tail skin temperature was measured with a thermo tracer after mice were subjected to a forced exercise task using a motor driven treadmill. In ovariectomized mice, forced exercise for 10 min was most effective in increasing tail skin temperature over that of sham-operated mice. This elevation was blocked by estradiol replacement (1 mg/kg per week for 3 weeks), suggesting that our model simulates menopausal hot flushes.

Keywords: ovariectomy, forced exercise, menopausal flushing

The menopausal hot flush is a bothersome symptom occurring in more than 75% of climacteric women (1). Manifesting as a transient increase in skin temperature and sweating hinders daily activity. Hot flushes have been linked to a transient disruption of the thermoregulatory mechanism that activates a heat-loss response including increased peripheral blood flow (2). Because hot flushes vary in duration, frequency, intensity, and duration of an individual flush, quantitative assessment of the disorder can be difficult (2). Flushing of the tail skin in ovariectomized (OVX) animals is known to be a good parameter of menopausal hot flushes, although the spontaneous appearance of flushing is irregular. Experimental manipulations including treatment with drugs trigger flushing in OVX-animals (3, 4). After morphine withdrawal with naloxone, a marked rise in tail skin temperature and an increase in heart rate appeared in OVX-rats (5). We previously demonstrated that nifedipine elevated tail skin temperature and that nifedipine-induced flushing was aggravated in mice with ovariectomy (6). This aggravation was blocked by estradiol replacement (6). In addition to drug-induced flushing, Rogers and Sheriff recently demonstrated that ovariectomy decreased hindlimb vascular conductance during graded mild-intensity treadmill locomotion in rats, this vascular modulation being reversed by estrogen replacement (7). Estrogen deficiency produces an abnormality of vascular tonus and/or insufficient autoregulation of the local vasculature. Therefore, we hypothesized that OVX-animals do not readily recover from forced exercise-increased peripheral vascular conductance. In the present study, we investigated changes in tail skin temperature before and after forced exercise on a motor-driven treadmill in OVX-mice as an experimental model of menopausal flushing.

Female ICR mice weighing 25 – 30 g were used (KyuDo Co., Ltd., Kumamoto). The mice were maintained on a 12-h light/dark schedule (lights on 7:00 a.m.) at a temperature of 24 ± 1°C with free access to food and water. All the procedures involving experimental animals adhered to the law (No. 105) and notification (No. 6) of the Japanese Government and were approved by the Laboratory Animal Care and Use Committee of Fukuoka University.

Mice underwent a bilateral ovariectomy or sham-operation under sodium pentobarbital anesthesia (50 mg /kg, i.p.) (6). Vehicle (sesame oil) and estradiol valerate (1.0 mg/kg) (Pelanin Depot; Mochida Pharmaceutical, Tokyo) were injected into the thigh muscle in a volume of 0.1 ml/100 g body weight once a week for 3 weeks starting 7 days after the operation. Twenty-eight days post-surgery, mice were subjected to the following

*Corresponding author. FAX: +81-92-862-2696
E-mail: ykataoka@cis.fukuoka-u.ac.jp

experiment in a room maintained at a temperature of 25 ± 1°C. The body weight in sham-mice, OVX-mice, and estradiol-treated OVX-mice were 31.0 ± 0.2, 34.0 ± 0.4, and 33.8 ± 0.2 g, respectively.

Tail skin temperature was measured according to a procedure described previously (6). Mice were restrained in a holder in a conscious state and the tail skin temperature was measured at the dorsal surface of the tail about 1 cm from its base with a thermo tracer (TH5108ME; NEC San-ei, Tokyo) for 15 min. The data were stored in 1-min blocks and analyzed with the Thermal Image processing program (TH51-701, NEC San-ei) and Remote Control program (TH51-723, NEC San-ei). Two hours after the basal tail skin temperature was measured, mice were forced to run (15 m/min) on a motor driven treadmill (MK-680S; Muromachi Kikai, Tokyo) for a period of 5, 10, or 20 min and the running time was measured. After termination of the forced exercise, tail skin temperature was measured for 15 min. Changes in tail skin temperature were assessed using ⊿TST. ⊿TST = (tail skin temperature in each 1-min block after the forced exercise) – (average basal tail skin temperature for the period from 1 to 6 min).

Values are expressed as the means ± S.E.M. Statistical analysis was performed using the two-way analysis of variance (ANOVA) followed by the Tukey-Kramer test. A value of $P<0.05$ was considered to be statistically significant. The intraobserver or interobserver variation was <5% in each experiment.

As shown in Fig. 1A, OVX-mice subjected to the forced exercise (10 min) showed rapid and marked increases in tail skin temperature, with a return to the basal level within 7 – 8 min. Meanwhile, sham-operated (sham) mice showed only slight increases in the early stage after forced exercise. Based on these time-courses of ⊿TST in sham- and OVX-mice (Fig. 1A), we evaluated the effect of forced exercise on tail skin temperature by accumulating ⊿TST for the period from 1 to 6 min after the forced exercise (total ⊿TST). Forced exercise for 10 and 20 min produced a marked increase in the total ⊿TST of OVX-mice compared to the sham-mice (Fig. 1B). The total ⊿TST of sham-mice increased with the amount of time the animals were forced to exercise. The difference in total ⊿TST between OVX- and sham-mice was the greatest (9.73 ± 1.06°C) after a 10-min period of forced exercise. The total running time of OVX-mice in each period was the same as that of sham-mice (inset of Fig. 1B). When OVX-mice were treated with estradiol valerate (1.0 mg/kg) once a week for 3 weeks, forced exercise-induced increases in total ⊿TST were markedly lowered by 81.3 ± 11.9% (Fig. 2A). In sham-mice, similar estradiol treatment did not influence the total ⊿TST and the running time after

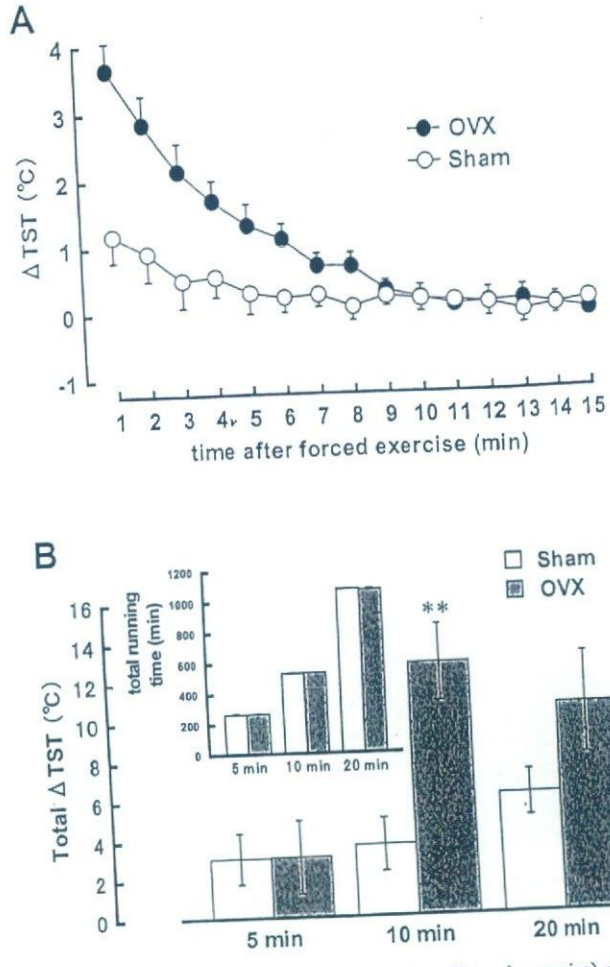

Fig. 1. Influence of treadmill locomotion (forced exercise) on tail skin temperature of sham-operated (sham) and ovariectomized (OVX) mice. A: Time course of changes in tail skin temperature (⊿TST) after forced exercise for 10 min. ⊿TST was calculated as follows: ⊿TST = (tail skin temperature in each 1-min block after the forced exercise) – (average basal tail skin temperature for the period from 1 to 6 min). B: Changes in accumulated ⊿TST and running time (inset of panel B) in the period from 1 to 6 min (total ⊿TST) after forced exercise for 5, 10, or 20 min in sham- and OVX-mice. Values represent the means ± S.E.M. for 5 to 7 animals. ** $P<0.01$, significant difference from sham-mice.

and during the forced exercise (10 or 20 min), respectively (data not shown). Representative thermograms show flushing of the tail skin in OVX-mice and estradiol-treated OVX-mice at 2 min after a 10-min period of forced exercise (Fig. 2B). There were no differences in running time between OVX-mice and estradiol-treated OVX-mice (inset of Fig. 2A).

In the present study, OVX-mice but not sham-mice showed a marked elevation in tail skin temperature at the early stage (1 to 6 min) after treadmill locomotion (15 m/min) for 10 min and this elevation was reversed by estrogen replacement. We propose that forced

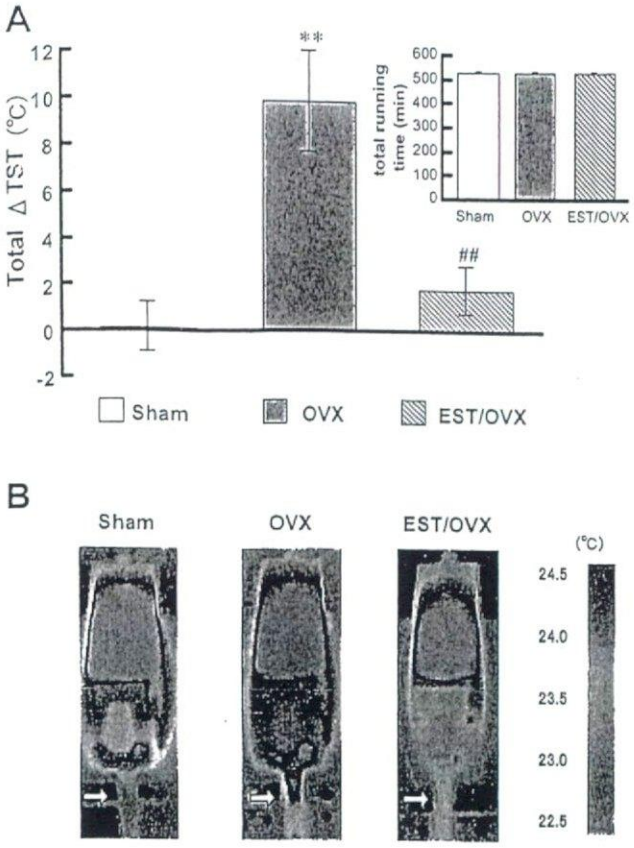

Fig. 2. Forced exercise-induced flushing of tail skin in mice with ovariectomy. A: Changes in tail skin temperature (total ΔTST) and total running time (inset of panel A) in the period from 1 to 6 min after forced exercise were induced by forced exercise for 10 min in sham-operated (sham) mice, ovariectomized (OVX) mice, and OVX-mice treated with estradiol (1 mg/kg) once a week for 3 weeks (EST/OVX). Values are the means ± S.E.M. for 10 to 13 animals. $^{**}P<0.01$ and $^{\#\#}P<0.01$, significant difference from sham- and OVX-mice, respectively. B: Representative thermograms showing flushing of the tail skin at 2 min after forced exercise (10 min) in sham-, OVX-, and EST/OVX-mice.

exercise-induced flushing of tail skin in OVX-mice is a conventional and useful experimental model of menopausal flushing. Changes in hindlimb vascular conductance during treadmill locomotion in OVX-rats were suggested to be positively associated with the production of endothelial nitric oxide (NO) (7). Chronic exercise increased the gene expression of endothelial NO synthase in canine aortic endothelial cells (8). Delp and Laughlin reported that levels of endothelial NO synthase protein in the aortas of rats increased after exercise training (9). Li et al. reported that basal NO generation is important in control of the cutaneous thermoregulatory microcirculation by ameliorating the arteriovenous anastomosis tone (10). These evidences together with the present findings suggest that the flushing of tail skin in OVX-rats is attributable to an insufficient vascular recovery from the vasodilatory response to forced exercise. Our previous findings demonstrated that ovariectomy significantly elevated the rise in tail skin temperature induced by nifedipine at a dose having no influence on blood pressure and that this event was blocked by estradiol replacement (6). Since estrogen promotes vascular relaxation and inhibits vascular contraction, the net result is a decrease in vascular resistance (11). It is, therefore, likely that estrogen deficiency leads to an abnormality of vascular tonus and/or insufficient autoregulation of the local vasculature. The protective effect of estrogen replacement in the present study may be related to an improvement of the abnormal local vascular tonus and autoregulation. On the other hand, calcitonin gene-related peptide (CGRP), a vasodilator neuropeptide is known to participate in the occurrence of menopausal hot flashes (12, 13). Recently, Noguchi et al. reported that ovariectomy not only potentiated CGRP-induced elevation of skin temperature and arterial vasorelaxation but also induced a lower concentration of endogenous CGRP in plasma and up-regulation of arterial CGRP receptors and that 17β-estradiol inhibited the CGRP-related responses in OVX-rats (14). Further studies are needed to clarify the CGRP-related mechanism in the present experimental model, forced exercise-induced flushing of tail skin in OVX-mice. Among sham-mice, OVX-mice, and estrogen-treated OVX-mice, there were no differences in the total running time during forced exercise (5, 10, and 20 min). This is consistent with the finding that changes in estrogen levels did not affect motor activity in rats (15). Therefore, the possibility that differences in forced exercise-induced flushing of the tail skin are due to changes in treadmill locomotion after estrogen withdrawal and/or estrogen replacement could be excluded.

In OVX-mice, flushing is detectable in the tail skin (3, 4), although experimental interventions are required for the induction of flushing. The present study demonstrated that forced exercise-induced flushing of tail skin in OVX-mice is a potentially useful experimental model of menopausal flushing.

Acknowledgments

This study was supported, in part, by a Grant-in-Aid for Scientific Research ((C)(2) 15590475) from JSPS and by a Grant-in-Aid for Exploratory Research (16659138) from MEXT, Japan.

References

1 Freedman RR. Physiology of hot flashes. Am J Human Biol. 2001;13:453–464.

2 Stearns V, Ullmer L, Lopez JF, Smith Y, Isaacs C, Hayes DF. Hot flushes. Lancet. 2002;360:1851–1861.
3 Dierschke DJ. Temperature changes suggestive of hot flushes in rhesus monkeys. J Med Primatol. 1985;14:271–280.
4 Kobayashi T, Tamura M, Hayashi M, Katsuura Y, Tanabe H, Ohta T, et al. Elevation of tail skin temperature in ovariectomized rats in relation to menopausal hot flushes. Am J Physiol Regulatory Integrative Comp Physiol. 2000:278:R863–R869.
5 Simpkins JW, Katovich MJ, Song IC. Similarities between morphine withdrawal in the rat and the menopausal hot flush. Life Sci. 1983;32:1957–1966.
6 Kai M, Tominaga K, Okimoto K, Yamauchi A, Kai H, Kataoka Y. Ovariectomy aggravates nifedipine-induced flushing of tail skin in mice. Eur J Pharmacol. 2003;481:79–82.
7 Rogers J, Sheriff DD. Role of estrogen in nitric oxide- and prostaglandin-dependent modulation of vascular conductance during treadmill locomotion in rats. Med Sci Sports Exerc. 2004;97:756–763.
8 Sessa WC, Pritchard K, Seyedi N, Wang J, Hintze TH. Chronic exercise in dogs increase coronary vascular nitric oxide production and endothelial cell nitric oxide synthase gene expression. Circ Res. 1993;73:829–838.
9 Delp MD, Laughlin MH. Time course of enhanced endothelium-mediated dilation in aora of trained rats. Med Sci Sports Exerc. 1997;29:1454–1461.
10 Li Z, Koman LA, Rosencrance E, Smith BP, Smith TL. Endogenous nitric oxide influences arteriovenous anastomosis adrenergic tone in the conscious rabbit ear. J Cardiovasc Pharmacol. 1998;32:349–356.
11 Austin CE. Chronic and acute effects of oestrogens on vascular contractility. J Hypertens. 2000;18:1365–1378.
12 Valentini A, Petrgia F, De Vita D, Nappi C, Margutti A, degli Uberti EC, et al. Changes of plasma calcitonin gene-related peptide levels in postmenopausal women. Am J Obstet Gynecol. 1996;175:638–642.
13 Wyon Y, Spetz AC, Theodorsson GE, Hammar ML. Concentration of calcitonin gene-related peptide and neuropeptide Y in plasma increase during flushes in postmenopausal women. Menopause. 2000;7:25–30.
14 Noguchi M, Ikarashi Y, Yuzurihara M, Kase Y, Chen JT, Takeda S, et al. Effects of the Japanese herbal medicine Keishi-Bukuryo-gan and 17β-estradiol on calcitonin gene-related peptide-induced elevation of skin temperature in overiectomized rats. J Endocrinol. 2003;176:359–366.
15 Zhang J, Inazu M, Tsuji K, Yamada E, Takeda H, Matsumiya T. Neurochemical characteristics and behavioral responses to psychological stress in ovariectomized rats. Pharmacol Res. 1999;39:455–461.

Cellular and Molecular Neurobiology, Vol. 25, No. 5, August 2005 (©2005)
DOI: 10.1007/s10571-005-4956-5

Short Communication

Cyclosporin A Aggravates Electroshock-Induced Convulsions in Mice with a Transient Middle Cerebral Artery Occlusion

Atsushi Yamauchi,[1] Hideki Shuto,[1] Shinya Dohgu,[1] Yoshitsugu Nakano,[1] Takashi Egawa,[1] and Yasufumi Kataoka[1,2]

Received January 11, 2005; accepted February 18, 2005

SUMMARY

1. To test whether an ischemic insult increases the susceptibility to cyclosporine A (CsA)-induced neurotoxicity, we examined the effect of CsA on the minimal electroshock-induced convulsions in mice treated with a transient middle cerebral artery occlusion (MCAO) for a short period (2 h).

2. This MCAO produced small to mid-sized infarcted regions in the cerebral hemisphere with increasing post-operative days. In MCAO mice, CsA (30 mg/kg, i.p.) elevated the incidence of minimal electroshock-induced convulsions to 90–100% over that in sham mice (20–30%) at 1–7 days but not 14 days post-surgery.

3. In light of these findings, the possibility that CsA increases the risk of convulsions in patients with cerebral infarction and/or at an early stage following focal cerebral ischemia would have to be considered.

KEY WORDS: cyclosporin A; electroshock-induced convulsions; middle cerebral artery occlusion; blood-brain barrier; mice.

INTRODUCTION

Cyclosporin A (CsA), an immunosuppressant, is widely used to prevent allograft rejection in solid organ transplantation and to treat various autoimmune diseases. CsA induces adverse events including renal, cardiovascular and gastrointestinal disorders. Neurological complications occur with a relatively high frequency (20–40%) (Gijitenbeek *et al.*, 1999; U. S. Group, 1994). The delivery of CsA into the brain is

[1] Department of Pharmaceutical Care and Health Sciences, Faculty of Pharmaceutical Sciences, Fukuoka University, 8-19-1 Nanakuma, Jonan-ku, Fukuoka 814-0180, Japan.
[2] To whom correspondence should be addressed; e-mail: ykataoka@cis.fukuoka-u.ac.jp.